AMMRC CTR 77-1

THE RELATIONSHIPS BETWEEN THE TRANSFORMATION CHARACTERISTICS AND THE FRACTURE AND FATIGUE PROPERTIES OF TRIP STEELS AND OTHER METASTABLE AUSTENITIC STEELS

JANUARY 1977

V. Weiss, K. Schroder, P. Sherman and A. Pan

Syracuse University, Department of Chemical Engineering and Materials Science, 409 Link Hall, Syracuse, New York 13210

Final Report Contract Number DAAG46-75-C-0065

Approved for public release; distribution unlimited

Prepared for

ARMY MATERIALS AND MECHANICS RESEARCH CENTER
Watertown, Massachusetts 02172

DISCLAIMER NOTICE

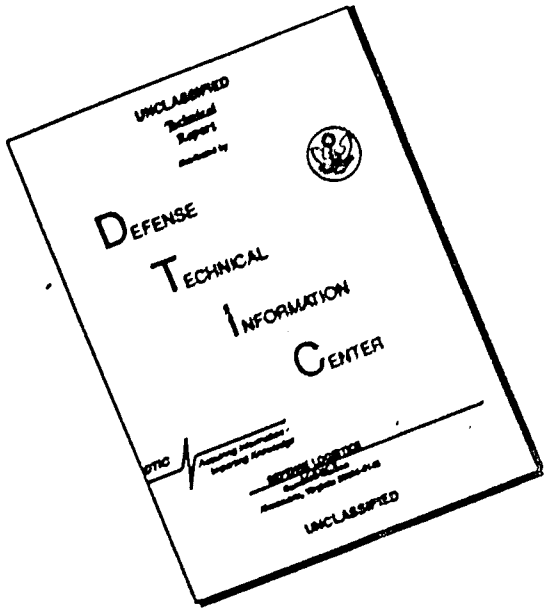

THIS DOCUMENT IS BEST QUALITY AVAILABLE. THE COPY FURNISHED TO DTIC CONTAINED A SIGNIFICANT NUMBER OF PAGES WHICH DO NOT REPRODUCE LEGIBLY.

The findings in this report are not to be construed as an official Department of the Army position, unless so designated by other authorized documents.

Mention of any trade names or manufacturers in this report shall not be construed as advertising nor as an official indorsement or approval of such products or companies by the United States Government.

DISPOSITION INSTRUCTIONS

Destroy this report when it is no longer needed.
Do not return it to the originator.

UNCLASSIFIED

SECURITY CLASSIFICATION OF THIS PAGE (When Data Entered)

REPORT DOCUMENTATION PAGE

READ INSTRUCTIONS BEFORE COMPLETING FORM

1. REPORT NUMBER: AMMRC CTR-77-1
2. GOVT ACCESSION NO.:
3. RECIPIENT'S CATALOG NUMBER:

4. TITLE (and Subtitle): THE RELATIONSHIPS BETWEEN THE TRANSFORMATION CHARACTERISTICS AND THE FRACTURE AND FATIGUE PROPERTIES OF TRIP STEELS AND OTHER METASTABLE AUSTENITIC STEELS

5. TYPE OF REPORT & PERIOD COVERED: FINAL REPORT

6. PERFORMING ORG. REPORT NUMBER:

7. AUTHOR(s): V. Weiss, K. Schroder, P. Sherman and A. Pan

8. CONTRACT OR GRANT NUMBER(s): DAAG46-75-C-0065

9. PERFORMING ORGANIZATION NAME AND ADDRESS: Syracuse University, Department of Chemical Engineering and Materials Science, 409 Link Hall Syracuse, New York, 13210

10. PROGRAM ELEMENT, PROJECT, TASK AREA & WORK UNIT NUMBERS: D/A Project: 1T162105AH84 AMCMS Code: 612105.11.148400 Agency Accession:

11. CONTROLLING OFFICE NAME AND ADDRESS: Army Materials and Mechanics Research Center Watertown, Massachusetts 02172

12. REPORT DATE: January 1977

13. NUMBER OF PAGES: 49 (61 p.)

14. MONITORING AGENCY NAME & ADDRESS (if different from Controlling Office):

15. SECURITY CLASS. (of this report): Unclassified

15a. DECLASSIFICATION/DOWNGRADING SCHEDULE:

16. DISTRIBUTION STATEMENT (of this Report)

Approved for public release; distribution unlimited.

17. DISTRIBUTION STATEMENT (of the abstract entered in Block 20, if different from Report)

18. SUPPLEMENTARY NOTES

19. KEY WORDS (Continue on reverse side if necessary and identify by block number)

TRIP steels
High strength steels
Stainless steels
Transformation plasticity
Phase transformation
Mechanical properties
Fatigue properties
Fracture toughness

20. ABSTRACT (Continue on reverse side if necessary and identify by block number)

Transformation plasticity was studied in TRIP steel wire, AM-355 CRT stainless steel sheet and two grades of type 301 stainless steel sheet. In the partially cold worked TRIP steel wire (yield strength 2070 MPa, tensile strength 2325 MPa) transformation plasticity is manifested by a martensite increase from 27% to 95% at fracture (ε_F=0.32, σ_F=4000 MPa) at room temperature The first stage of martensite formation occurs during plastic straining to 0.04 - 0.1 when the martensite increases from 27% to 70%. Further straining to fracture, within less than two wire diameters gage length, causes further

DD FORM 1 JAN 73 1473 EDITION OF 1 NOV 65 IS OBSOLETE

UNCLASSIFIED

SECURITY CLASSIFICATION OF THIS PAGE (When Data Entered)

406796

transformation to nearly 100% martensite. The rotating beam fatigue endurance limit (1350 MPa) is higher than anticipated from the tensile strength, probably due to a significant amount of martensite formation in the failure zone. No martensite is formed for tension-tension cycling for 10,000 cycles and maximum stresses up to 862 MPa.

For AM-355 CRT the fracture ductility decreases with increasing stress biaxiality from 0.6 for uniaxial tension to 0.2 for plane strain tension and bulge tests. In the bulge test the martensite content increases from 45 to 85% for a strain of 0.2. Increasing the strain rate causes an increase in the bulge ductility to 0.5 for explosive tests ($\dot{\varepsilon} \sim 10^3$ sec^{-1}). The plane stress fracture toughness for AM-355 CRT was measured as approximately 110 MNm$^{-3/2}$ with the formation of approximately 20% martensite near the crack zone.

Type 301 stainless steel (half hard grade) also showed significant increase in bulge ductility with increasing strain rate from 0.4 under quasi static loading to 0.8 under explosive loading ($\dot{\varepsilon} \sim 10^3$ sec^{-4}) with a concomitant martensite transformation from approximately 20% to over 90%.

FOREWORD

This report contains the findings of a research program entitled, "The Relationships Between the Transformation Characteristics and the Fracture and Fatigue Properties of TRIP Steels and Other Metastable Austenitic Steels" under contract number DAAG-75-C-0065 with Dr. M. Azrin of Army Materials and Mechanics Research Center serving as Contracting Officer. The study was conducted in Syracuse University's Department of Chemical Engineering and Materials Science under the direction of Dr. Volker Weiss, Professor of Materials Science.

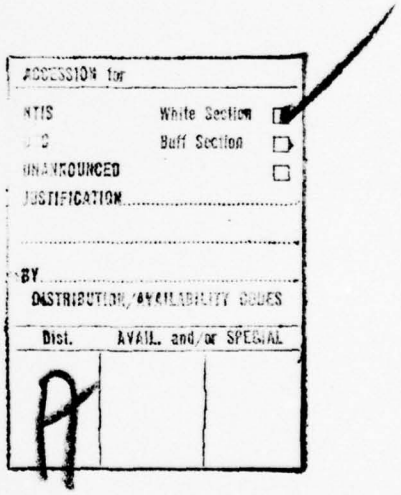

THE RELATIONSHIPS BETWEEN THE TRANSFORMATION CHARACTERISTICS AND THE FRACTURE AND FATIGUE PROPERTIES OF TRIP STEELS AND OTHER METASTABLE AUSTENITIC STEELS

ABSTRACT

Transformation plasticity was studied in TRIP steel wire, AM-355 CRT stainless steel sheet and two grades of type 301 stainless steel sheet. In the partially cold worked TRIP steel wire (yield strength 2070 MPa, tensile strength 2325 MPa) transformation plasticity is manifested by a martensite increase from 27% to 95% at fracture ($\varepsilon_F = 0.32$, $\sigma_F = 4000$ MPa) at room temperature. The first stage of martensite formation occurs during plastic straining to 0.04 - 0.1 when the martensite increases from 27% to 70%. Further straining to fracture, within less than two wire diameters gage length, causes further transformation to nearly 100% martensite. The rotating beam fatigue endurance limit (1350 MPa) is higher than anticipated from the tensile strength, probably due to a significant amount of martensite formation in the failure zone. No martensite is formed for tension-tension cycling for 10,000 cycles and maximum stresses up to 862 MPa.

For AM-355 CRT the fracture ductility decreases with increasing stress biaxiality from 0.6 for uniaxial tension to 0.2 for plane strain tension and bulge tests. In the bulge test the martensite content increases from 45 to 85% for a strain of 0.2. Increasing the strain rate causes an increase in the bulge ductility to 0.5 for explosive tests ($\dot{\varepsilon} \sim 10^3$ sec^{-1}). The plane stress fracture toughness for AM-355 CRT was measured as approximately 110 MNm $^{-3/2}$ with the formation of approximately 20% martensite near the crack zone.

Type 301 stainless steel (half hard grade) also showed significant increase in bulge ductility with increasing strain rate from 0.4 under quasi static loading to 0.8 under explosive loading ($\dot{\varepsilon} \sim 10^3$ sec^{-1}) with a concomitant martensite transformation from approximately 20% to over 90%.

ACKNOWLEDGEMENT

The authors gratefully acknowledge the support of AMMRC, for supplying the TRIP steel wire, and thank especially Drs. Larson and Azrin for their continued guidance. They also wish to thank Allegheny Ludlum Steel Corporation for supplying the AM-355 CRT steel sheet.

LIST OF FIGURES

LIST OF TABLES

I. INTRODUCTION

High stress transformation plasticity offers a means of increasing the strength as well as the ductility and toughness of steels (1,2). Prior studies at Syracuse University (3), AMMRC (4), and at the University of California at Berkeley (1) have shown that an optimum combination of strength and toughness or fatigue crack growth resistance requires careful control of phase metastability with respect to the service conditions. For example, a TRIP steel that exhibits high strength and toughness under relatively low strain rates at room temperature may suffer a significant loss of uniform ductility at very high strain rates (5). Also the same TRIP steel may be inferior in fatigue crack propagation resistance to an ultra high strength steel.

The present study was aimed at obtaining further information on the inter-relationships between the microstructural, composition, and the mechanical variables. Of particular interest were the stress-strain-martensite relations for various strain rates, the effect of stress state on these relationships and the kinetics of martensite formation under fatigue conditions.

Unfortunately, TRIP steel was only available in wire form. Thus only the uniaxial tensile tests and the rotating beam fatigue tests were conducted on this material. The effects of strain rate on tensile strength and elongation for TRIP steel wires were determined by the manufacturer and are also reported here (Appendix). To obtain the effect of stress state on the strain-martensite-ductility relationships in metastable austenitic alloys, tests were conducted on type 301 stainless steel and on AM-355 CRT steel. While these steels do not achieve the strength level of TRIP steels, it is believed that the results can be used as a guide to estimate the stress state effects on TRIP steel.

II. MATERIALS

Three metastable steels were used in the present study. The TRIP steel was available in 0.056, 0.054 and 0.041 inch (1.42, 1.37 and 1.04 mm) diameter wire. The monotonic tension studies, the effect of deformation temperature and the fatigue studies were conducted on this material. The other two materials were commercially available Type 301 stainless steel and AM-355 CRT. The chemical composition and other information are listed in Table I.

The AM-355 CRT samples were processed by solution annealing followed by 30% cold rolling and a tempering-aging treatment at 800°F (427°C) for three hours. The TRIP steel rod was austenized at 2000°F (1095°C), quenched and then warm drawn to produce it in the wire form. The wire was warm drawn (from a 0.150 inch diameter rod) at 800°F to 0.060-inch diameter

for the making of 0.056-inch diameter wire and to 0.058 for drawing to 0.054-inches. This drawing was done in eight equal passes. The 0.056-inch diameter wire was cold drawn from 0.060-inch diameter. The 0.054-inch diameter wire was cold drawn from 0.058-inch diameter. For the final process of the 0.041-inch diameter wire, the wire was warm drawn from a 0.115-inch diameter to 0.044-inch diameter. The 0.044-inch wire was then cold drawn to 0.041-inches. The purpose of the final cold-working step was to raise the yield strength above 300 ksi by the formation of martensite. No heat treatment history was available for the Type 301 stainless steel sheet, except that one lot had been cold rolled to produce approximately 21 percent to 28 percent and the other to produce 83 to 84 percent martensite, probably corresponding to the half hard and the fully hard condition, respectively.

III. MARTENSITE DETERMINATION

Depending on the specimen type and test program the martensite content was determined by a) destructive metallography, b) X-ray diffraction, c) magne gage and d) a vibrating magnetometer. All except the last of the techniques mentioned here are standard techniques; they are well documented and have been described in an earlier report (3).

The total magentization of small wire sections was determined in a vibrating magentometer. This instrument was built following a design by Foner (6). Essentially, a sample vibrates in a magnetic field. Its oscillation induces a voltage in coils in the neighborhood of the sample. This voltage is amplified in a lock-in-amplifier, which is connected electrically in such a way to the vibrator of the sample that only signals in a fixed phase and frequency in relation to the vibration of the sample will be amplified. Figure 1 gives a schematic diagram of the experimental system. The sample and a reference magnet are driven by the oscillatory movement of a loudspeaker. The amplitude of vibration is monitored and kept constant by keeping the signal from a second coil, in which the reference magnet oscillates, constant. The output signal from the pickup coils is therefore proportional to the magnetic moment of the sample.

The magnetometer was calibrated with a small high purity iron sample with volume V in the field range above 8 kOe in which the M-H curve is flat, indicating that saturation was reached. This calibration gives the value of "(dipole moment of the sample $\mu = I_s \cdot V$)/(voltage output of lock-in-amplifier)". Then the magnetic moment $I_s = \mu/V$ of TRIP steel wire sections was determined. The saturation magnetization I_s of the martensite in TRIP steel is not known. One would expect that it should be lower than that of α-iron due to the non-ferromagnetic alloying elements. This TRIP steel has 15% of chromium and 6% of other nonferromagnetic impurities. Ferromagnetic impurities are 13.35% cobalt and 1.5% nickel. The saturation moment I_s of the TRIP steel martensite can be calculated in the following way. One determines first I_s of an alloy which has only the ferromagnetic

components in the same ratio as found in the TRIP steel ($m_{Co} : m_{Ni} : m_{Fe} = 13.35 : 1.5 : 64$). Its saturation magnetization is about 5% higher than that of α-Fe. 15% chromium in iron leads to a reduction of I_s by 19%. About the same reduction should be found in the TRIP steel. The reduction of I_s can be described approximately by assuming that the non-ferromagnetic impurity replaces a ferromagnetic Fe- or Co-atom in the lattice. This means that the 5.1 w/o Mo ≃ 3 at/0 Mo reduces I_s by an additional 3%. The remaining non-magnetic impurities (about 1%) should reduce I_s by another 1%. Therefore I_s (TRIP steel martensite)/I_s (α-Fe) = 0.81 within 1 to 2%. thus the amount of martensite in a given sample is obtained from

$$\% \text{ Martensite} = \frac{(I_{\text{TS sample}}/0.81)}{I_{\alpha\text{Fe reference}}}$$

where the magnetic moment ratio ($I_{\text{TS sample}}/I_{\alpha\text{Fe reference}}$) is obtained from the respective output voltage ratios.

The magnetic field was 12 kOe. This insured that the saturation magnetization was measured. The magnetization was normalized with respect to the sample weight. The concentration of martensite, which is proportional to the magnetization per gram, can then be found.

IV. EXPERIMENTAL RESULTS AND DISCUSSION

I. Tension Tests

A. TRIP Steel

The true stress-strain diagram and martensite-strain diagram for 0.056-inch (1.4 mm) diameter TRIP steel wire having a 1-inch (25.4 mm) gage length is shown in Figure 2. As the wire was already pre-strained at room temperature 14 percent, which produced approximately 27 percent martensite, no yield drop or Luders strain is observed. The tensile strength is 320 ksi (2400 MPa), the 0.2% yield strength 280 ksi (1930 MPa). The elongation was 13 percent. These results are in substantial agreement with the data obtained by the Crucible Special Metals Division of Colt Industries and given in the Appendix. Another tension test was performed on a specimen having a 10-inch (254 mm) gage length. The results are presented in Table II. The tensile strength was 302 ksi (2093 MPa), the elongation in 10-inches (254 mm) was 7.18 percent and the true fracture strain was 0.32. These data are also in reasonable agreement with the data given in the Appendix.

A-1 Martensite Content vs. Percent True Strain

To produce a strain in the TRIP steel wire, a tensile load was applied until either 1) a section of the wire had undergone diameter reduction as found by micrometer measurements, or 2) fracture occurred.

If the first case occurred the specimen was unloaded and removed from its holders. A small length, about 0.25-inch (6mm), of the strained wire which had a constant new diameter was then cut from the specimen. In the second case the fractured specimen was examined with a micrometer for length sections with a constant diameter. Such length sections were cut from the specimens.

By these methods we obtained lengths corresponding to true strains of 3.5 percent, 7.2 percent, 11.0 percent and 14.7 percent as well as an original specimen of zero strain. The vibrating magnetometer was then used to obtain the martensite content of each section. The results of these measurements are shown in Figure 3. The as-received wire had a martensite content of approximately 25 percent. Straining to 5 percent caused an increase in martensite content to approximately 75%. Further straining seemed to cause little additional martensite formation, except at the location closest to the fracture where the vibrating magnetometer indicated 95% martensite.

A number of wire sections were strained to failure at elevated temperatures. TRIP steel wires of diameter 0.056-inches (and length approximately 20-inches) were held in a Baldwin Testing machine. A section of the wire approximately 1 cm long was polished to a diameter of 0.054-inch with grit 240 sandpaper. This insured failure within that length rather than at the grip edges. A Chromel-Alumel thermocouple was then spot welded in that thinned length and the TRIP steel wire was enclosed in a 16-inch oven. Specimens which failed at the spot weld were disregarded. The Variac provided control for the oven current and shunts were used to provide stability of temperature in the test length. The reduced length where fracture occurred was kept within $\pm$ 10°F as determined by three attached thermocouples. When the test temperature was reached (about 15 minutes) the load was applied until failure occurred.

The martensite was measured in the first 0.25 inch (6mm) of failure location, thus representing near maximum martensite formation achievable in this material as a function of test temperature. The results are given in Figure 4. The martensite content decreases from 95 percent at room temperature to 40 percent at 700°F (370°C). A rapid decrease in transformed martensite is found to exist between the deformed TRIP steel at room temperature and 300°F (150°C).

A-2 Hardness Studies

Vickers micro-hardness tests (7) were conducted on TRIP steel wires as a function of distance from the fracture location. The specimens tested were mounted in a bakelite mold and polished to midthickness. The indentation load was 60 grams (0.59N) and held for 10 seconds. The specimens were those tested at room temperature and 500°F (260°C). The results are shown in Figure 5.

A first order least squares fit yields a Vickers hardness value of 646.4 at the fracture surface of the room temperature tested specimen and a value of 602.5 at the fracture surface of the 500°F (260°C) tested specimen.

B. AM-355 CRT

Uniaxial tension tests in the longitudinal and transverse directions with respect to the rolling direction, were conducted on sheet specimens of geometry as shown in Figure 6 on AM-355 stainless steel. The effective strain is defined as

$$\bar{\varepsilon}_F = \varepsilon_{1F} = \ln \frac{A_o}{A_F}$$

where A_o is the initial cross section area and A_F is the final cross section area. Detailed results of four specimens tested are given in Table III. Good agreement is found with the data supplied by the manufacturer, Allegheny Ludlum.

II. Multiaxial Tests

Plane strain tension tests (Figure 7), plane strain bend tests (Figure 8), hydraulic bulge tests (Figure 9), miniature bulge tests (Figure 10) and explosive bulge tests (Figure 11) have been conducted on AM-355 CRT and Type 301 stainless steels. In the plane strain tension test a stress biaxiality $\sigma_2/\sigma_1 = 1/2$ is obtained at the center section of the groove (8). In this case the effective fracture strain is given by

$$\bar{\varepsilon}_F = \frac{2}{\sqrt{3}} \varepsilon_{1F} , \qquad \varepsilon_{2F} = 0$$

$$\varepsilon_{1F} = - \varepsilon_{3F} = - \ln \frac{t_f}{t_i}$$

where t_i is the initial thickness and t_f the final thickness.

In the plane strain bend test, bending of wide specimens over a cylindrical die was used to determine the plane strain ductility value ($\sigma_2/\sigma_1 = 1/2$, $\sigma_3 = 0$), Figure 8. It has been demonstrated (9) that plane strain conditions are obtained at the center section of the top and bottom surfaces of a bend specimen for width to thickness ratios in excess of 8. For the present test series, a specimen geometry having a width to thickness ratio of 10 was chosen. This test was done on AM-355 CRT stainless steel. The test is essentially a three point bend test with a side clearance of approximately one sheet thickness once the specimen has achieved a "U" bend over the cylindrical dowel. To minimize friction teflon tape was inserted under the mandrel and between the edge supports and the specimen. The fracture strain was designated as that strain at the onset of surface cracking. The effective strain in this case is given by

$$\bar{\varepsilon}_F = \frac{2}{\sqrt{3}} \varepsilon_{1F} \qquad \text{since} \qquad \varepsilon_{3F} = 0 , \qquad \varepsilon_{1F} = \varepsilon_{2F}$$

If the sheet specimen is bent over a cylinder of diameter D, ε_{1F} is

$$\varepsilon_{1F} = \ln\left(1 + \frac{t}{D+t}\right)$$

where t is the specimen thickness. In the center of the outer surface of the bend specimen $\varepsilon_{3F} = 0$, $\varepsilon_{1F} = -\varepsilon_{2F}$.

Hydraulic bulge tests were done on 301 stainless steel with thickness of .0256-inch (0.65 mm). The basic components of the bulge fixture are shown in Figure 9. It essentially consists of the pressure cylinder with hydraulic oil, a piston and the top support. The specimen, along with the cylinder and the top support, is held in position between two flanges. In order to prevent leakage of oil during testing O-rings are provided between the specimen and the pressure cylinder. To pressurize the cylinder the piston is connected with the moving plate of the Baldwin Testing Machine. The tests were done with different crosshead speed ranging from 0.001 in/min to 0.3 in/min (0.03 mm/min to 7.6 mm/min).

The test fixture for the miniature bulge test was modelled after a design by Azrin and Backofen (10) and is shown in Figure 10. The test consisted of pushing a spherical ball against a 2-inch x 2-inch (50.8 mm x 50.8 mm) (Figure 12) sheet specimen by means of a dowel having the capacity to hold variable sizes of balls. A teflon spacer is placed between the ball and the specimen so that the central test section remains free of any contact with the loading tool. These tests were done on 1) AM-355 CRT sheet as received, 2) AM-355 CRT sheet with one side wet ground 0.019-inch (0.48 mm) off, and 3) 301 stainless steel with different crosshead speed. The stress state in the test section is truly biaxial in nature. The effective fracture strain is given by

$$\bar{\varepsilon}_F = -\varepsilon_{3F} = \ln\frac{t_f}{t_i}$$

$$\varepsilon_F = \varepsilon_{2F} = -\frac{\varepsilon_{3F}}{2}$$

where t_i is the initial thickness and t_f is the final thickness of the test area.

Explosive bulge tests were conducted on AM-355 CRT and 301 stainless steel by the system developed by Biegel (11). It is essentially a hydraulic bulge test activated by the explosive pressure of gun powder with a 150,000 psi maximum. The strain rate is estimated to be $5 \times 10^3 - 6 \times 10^3$ sec^{-1}. This strain rate is estimated by consideration of the duration of the explosive test (approximately 0.1 to 1 microsecond) and the effective strain measured after the test. The results for AM-355 CRT, Tables IV, V and VI, show the decrease in fracture ductility with increasing stress

biaxiality, Figure 13. Variations are largely due to the fact that the martensite content of AM-355 CRT varied from the surface of the sheet towards the center, Figure 14. Specimens that required considerable surface removal generally showed higher fracture ductilities. While the center of the sheet had an average martensite content of 40 percent the surface was practically 100 percent martensite, decreasing linearly to the center value within approximately 0.020-inch (0.5 mm). For the plane strain tension test and the miniature bulge test the amount of transformation during the straining to fracture ($\dot{\varepsilon}_F = 0.2$) is between 30 and 50 percent, when measured in the center of the test specimen. The martensite data shown in Table IV, were obtained on the surface and are thus not representative of the bulk. The martensite formation in AM-355 CRT during the plane strain bend tests was negligible since the measurements were made at the surface where the martensite content was nearly 100 percent.

The effect of strain rate on the bulge ductility of AM-355 CRT is shown in Figure 15. The bulge ductility increases significantly with strain rate from 0.17 for the static test to approximately .50 for the explosive bulge test having a strain rate of approximately $10^3 \cdot \text{sec}^{-1}$. The amount of martensite formation also increases with increasing strain rate from around 40 percent for the slow hydraulic bulge test to over 50 percent for the explosive bulge test. The results are also presented in Tables V and VI.

Fracture toughness tests were conducted on AM-355 CRT compact tension specimens (Figure 16) with 0.1-inch (2.54 mm) thickness as received and 0.06-inch (1.52 mm) wet ground. The material thickness was not adequate to qualify the tests as valid K_{Ic} tests. The apparent toughness values were calculated according to (12)

$$K_a = \frac{P_Q}{t\sqrt{w}} \; F\left(\frac{a}{w}\right)$$

where P_Q represents the load for 5 percent secant offset; t = thickness; w = width; and a is the crack length of the specimen. The value of the function F(a/w) was obtained from the listed Table (12) for the ratio a/w.

The results are given in Table VII. The apparent fracture toughness was approximately 100 $\text{ksi}\sqrt{\text{in}}$(110 $\text{MNm}^{-3/2}$). The amount of martensite formation, measured near the crack path again depends on the specimen preparation, i.e., on the amount of surface removal during specimen preparation. From the results of specimen number 3 (Table VII), it can be estimated that approximately 20 percent martensite is formed during deformation in the near-crack zone.

Weiss and co-workers have recently shown (13) correlations between the fracture toughness and the bulge ductility. According to these findings the plane strain fracture toughness is related to the bulge ductility by:

$$K_{Ic} = 147 \cdot \varepsilon_{F\ \text{Bulge}}\ \text{ksi}\ \sqrt{\text{in}}$$

$$K_{Ic} = 162 \cdot \varepsilon_{F\ Bulge}\ MNm^{-3/2}$$

The plane stress fracture toughness is approximately 3.6 times the plane strain fracture toughness given by the above relations, i.e., $K_c = 580\ \bar{\varepsilon}_{F\ Bulge}\ MNm^{-3/2}$. The bulge ductility value for AM-355 CRT obtained under quasi static conditions, 0.17, yields an estimate for the plane stress fracture toughness of approximately 90 ksi$\sqrt{in}$ which is in fair agreement with the experimental value of K_c.

The bulge test results for type 301 stainless steel are given in Tables VI, VIII and IX and in Figure 17. The test program on this material was principally aimed at studying the effect of strain rate on the bulge ductility and the concurrent martensite formation. Figure 17 shows the increase in bulge ductility, i.e., the effective true fracture stain under an equi-biaxial stress state, from approximately 0.3 under quasi static conditions to above 0.7 under explosive conditions, i.e., $\dot{\varepsilon} \simeq 10^3\ sec^{-1}$. The amount of martensite formation is around 10 - 15 percent from approximately 84 percent martensite in the as-received condition for the fully hardened type 301 stainless steel.

III. Fatigue Tests

Fatigue tests were conducted on TRIP steel wire using a R. R. Moore High Speed Fatigue Testing Machine which was modified to accommodate 0.056-inch (1.42 mm) diameter wire.

The R. R. Moore Fatigue Testing Machine is of the rotating beam type, and consists essentially of two housings, each of which supports a rotating spindle. When rotated one half revolution the stress in the fiber originally above the neutral axis of the specimen are reversed from compression to tension of equal intensity. Upon completing the revolution, the stresses are again reversed, so that during one complete revolution the test specimen passes through a complete cycle of flexural stress.

The housings are supported on trunnions which permit deflections of the housings in a vertical plane when the load is applied. Knife edge seats mounted on opposite sides of each housing receive the knife edges mounted on the ends of the hanger yoke which carries the load weight. The load consists of accurately adjusted weights stacked on the weight hanger.

It was necessary to counter balance the weight of the bearing housings with a lead weight, as shown in Figure 18, since the housing weight will cause a fiber stress on the wire.

Pin vises were modified to fit in the bearing housings as shown in Figure 19. To insure failure in the gage length, the wire was sanded while running in the machine at zero load. This provided a contoured specimen with a minimum diameter in the gage length. It was usually necessary to reduce the wire diameter from 0.056-inch (1.42 mm) to 0.042-inch (1.07 mm).

The extreme fiber stress was determined by the relation

$$S = \frac{16WL}{\pi D^3}$$

where S = extreme fiber stress (PSI)

W = total load on specimen (Pounds)

L = moment arm (distance from end support to load point) (fixed at 4 inches)

D = minimum diameter of specimen (inches)

Using this equation, the alternating stress on the wire specimens was determined and the S-N curve for the TRIP steel wire was determined, Figure 20. A fatigue limit of approximately 200 ksi (1380 MPa) was determined.

In a separate test program TRIP steel wire sections were subjected to tension-tension cycling ($R \sim 0.1$) at various stress ranges. These tests were not run to failure but stopped after 10,000 cycles where the specimen was removed for martensite measurement. The results are shown in Figure 21. It can be concluded that no apparent increase in martensite occurs during fatigue for maximum cyclic stress up to 860 MPa after 10,000 cycles. The fact that the initial concentration of martensite for the TRIP steel in the as-received state in Figure 21 differs significantly from the wire in the as-received state in Figure 2 inclines us to suspect that the martensite formation in the cold drawing of the TRIP steel wire is not uniform.

V. SUMMARY

Transformation plasticity was studied in TRIP steel, AM-355 CRT stainless steel and type 301 stainless steel.

In the TRIP steel wire, which was partially cold rolled and contained approximately 20 percent martensite, the martensite content rose rapidly to about 70 percent when strained at room temperature to about 5 percent. Straining from 5 to 15 percent caused little additional martensite formation. However, further straining to the fracture strain, 0.32, yielded an almost completely martensitic structure. The martensite content at the fracture strain is a function of the test temperature and decreases from 95 percent at room temperature 20°C, to approximately 42 percent at 380°C. For the room temperature tests, the microhardness distribution near the fracture surface indicates that the martensite content increases from $\sim$ 60 percent at the strains between 0.04 and 0.1 to 100 percent at the fracture surface within less than 1 wire diameter (1.4 mm). Rotating beam fatigue studies show an endurance limit of approximately 1380 MPa at around 10^6 to 10^7 cycles. Martensite formation in fatigue, even in homogeneous tension

tension cycling, is apparently a completely local phenomenon. No change in martensite content was observed for maximum cycle stresses up to 862 MPa after 10,000 cycles.

AM-355 CRT was studied to determine the role of stress state and strain rate on high stress transformation plasticity. The stress state effect on fracture strain is similar to that of high strength microstructure stable materials and follows the critical mean stress criterion proposed by Weiss (14). The ductility decreases from 0.6 in tension to 0.2 in plane strain bending and in the plane strain tension test and under equibiaxial stresses in the bulge test. In the bulge test specimens the martensite increase in the center section of the sheet is from approximately 40 percent to approximately 85 percent. Under equibiaxial conditions the fracture strain increases with increasing strain rate from 0.2 for quasi static conditions to 0.5 for explosive bulging, $\dot{\bar{\varepsilon}} = 10^3\ \text{sec}^{-1}$. The apparent (plane stress) fracture toughness for AM-355 CRT is approximately 110 $\text{MNm}^{-3/2}$. This is in agreement with the plane stress correlation between bulge ductility and fracture toughness developed by Weiss and co-workers (13), namely $K_c = 580 \cdot \bar{\varepsilon}_{F\ \text{Bulge}} \cdot \text{MNm}^{-3/2}$.

Type 301 stainless steel was also included to study the effect of strain rate on the bulge ductility. Again a significant increase is observed with increasing strain rate from 0.4 under quasi static conditions to 0.8 under explosive conditions ($\dot{\bar{\varepsilon}} \simeq 10^3\ \text{sec}^{-1}$). For this almost fully hard 301 stainless steel the concomitant martensite formation is approximately 15 percent.

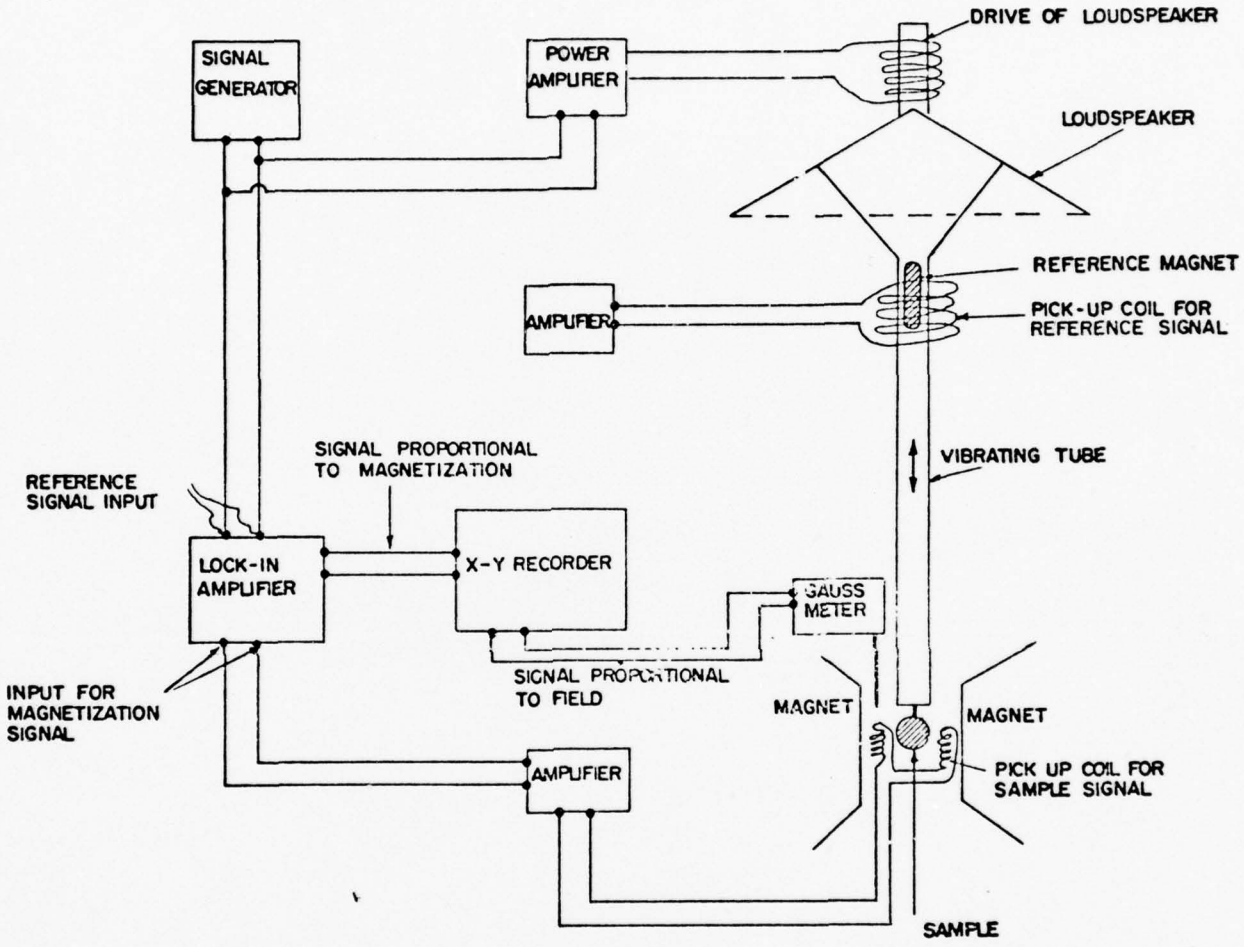

FIG. 1. SCHEMATIC DIAGRAM OF VIBRATING MAGNETOMETER.

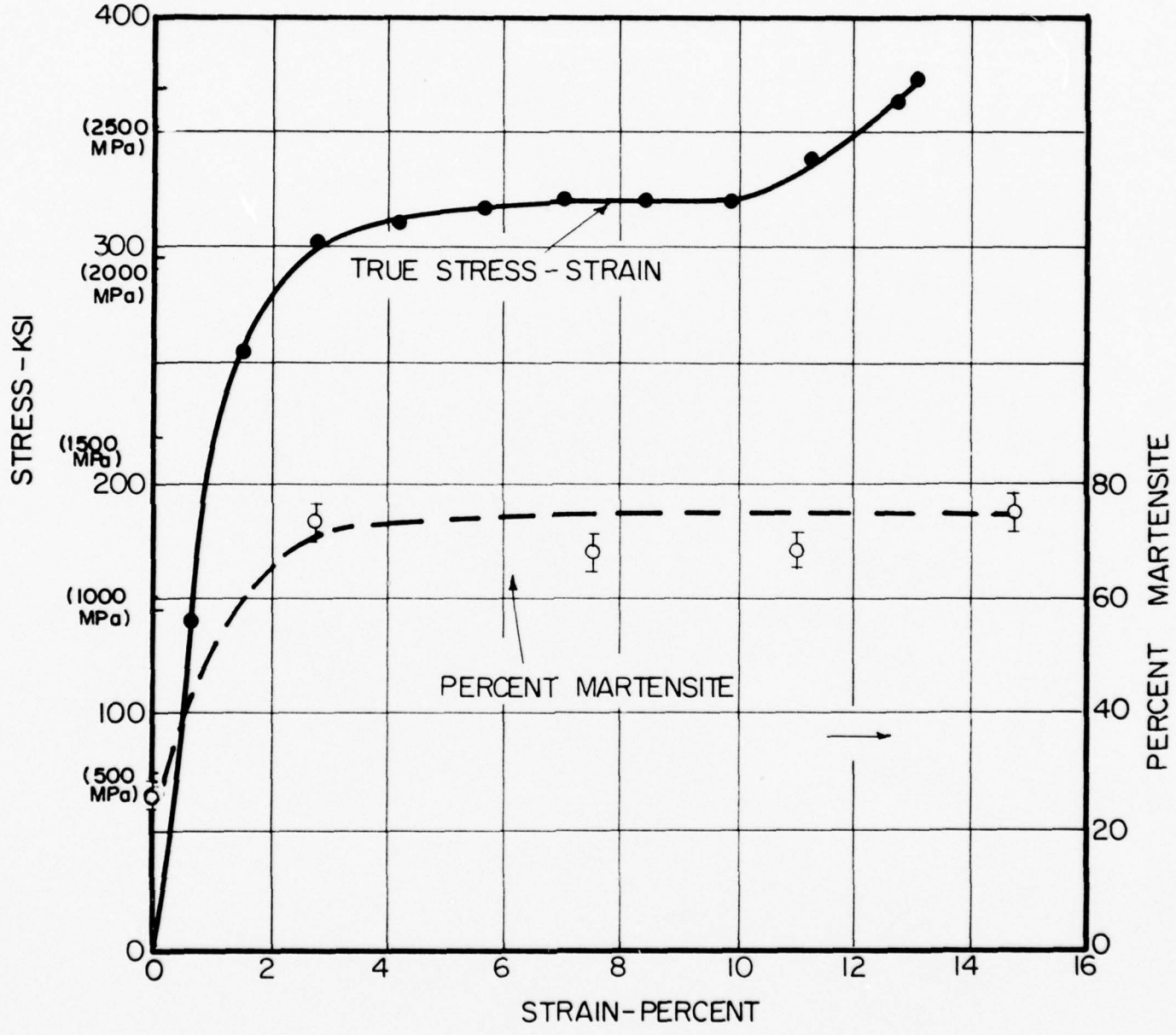

FIGURE 2. TRUE STRESS STRAIN DIAGRAM AND MARTENSITE-STRAIN DIAGRAM FOR 0.056 INCH DIAMETER TRIP STEEL WIRE. TESTS WERE CONDUCTED AT ROOM TEMPERATURE.

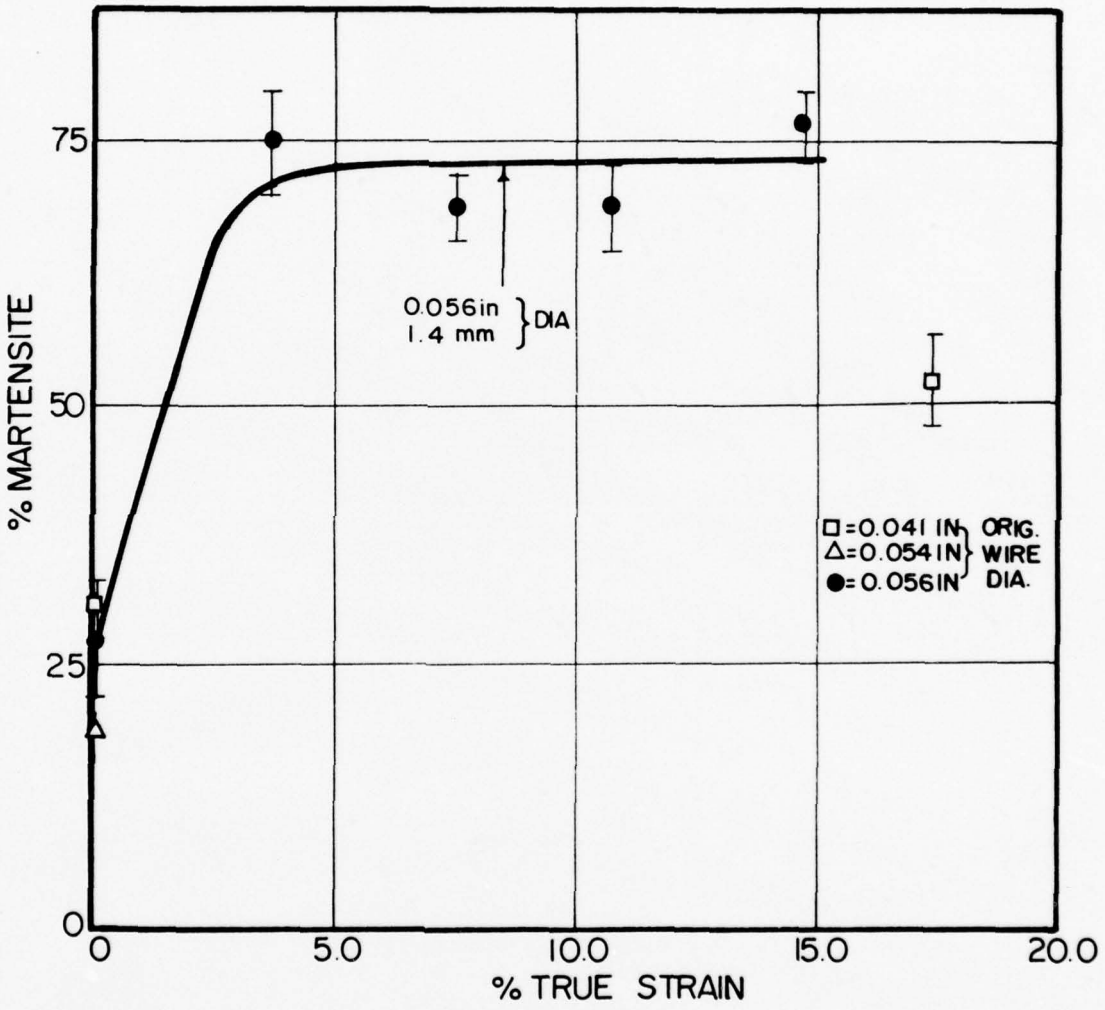

FIG. 3. MARTENSITE CONTENT VS. PERCENT TRUE STRAIN FOR TRIP STEEL WIRE (MEASURED ON DIFFERENT WIRE SECTIONS).

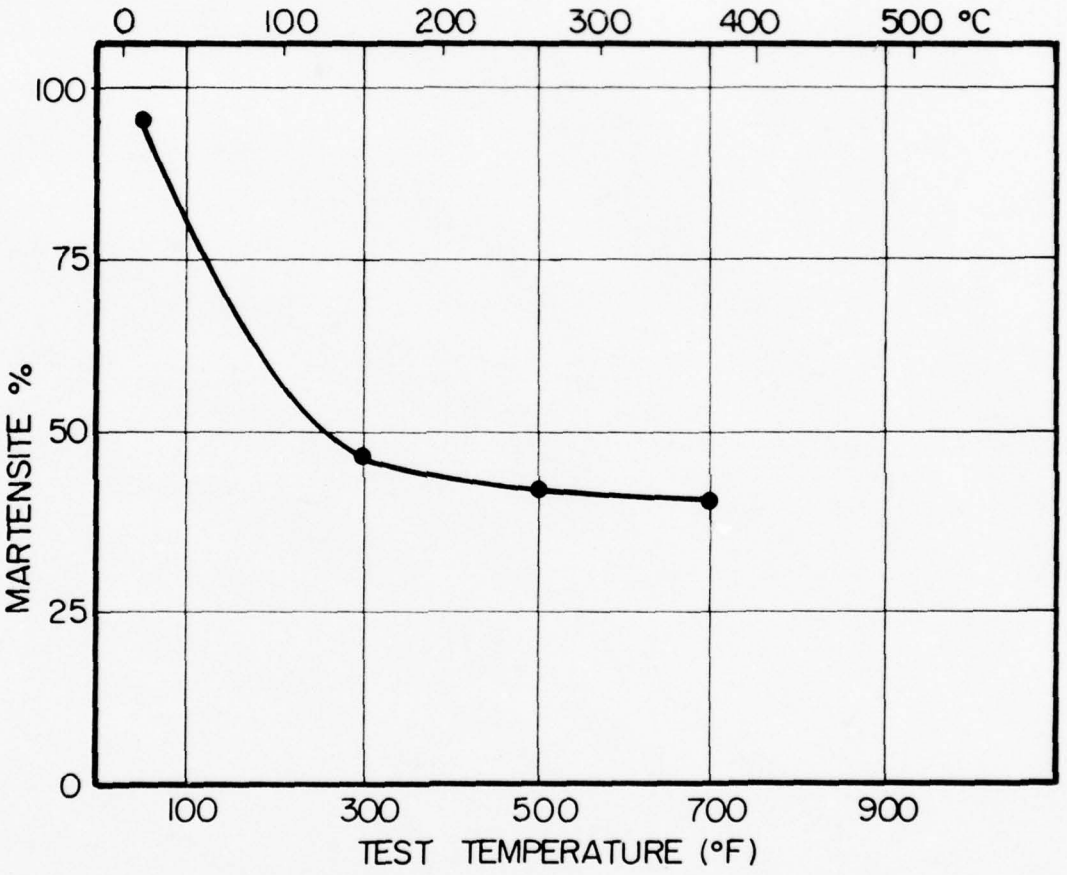

FIG. 4. MARTENSITE CONTENT NEAR THE FRACTURE SURFACE FOR 0.056-INCH TRIP STEEL WIRE VS. TEST TEMPERATURE.

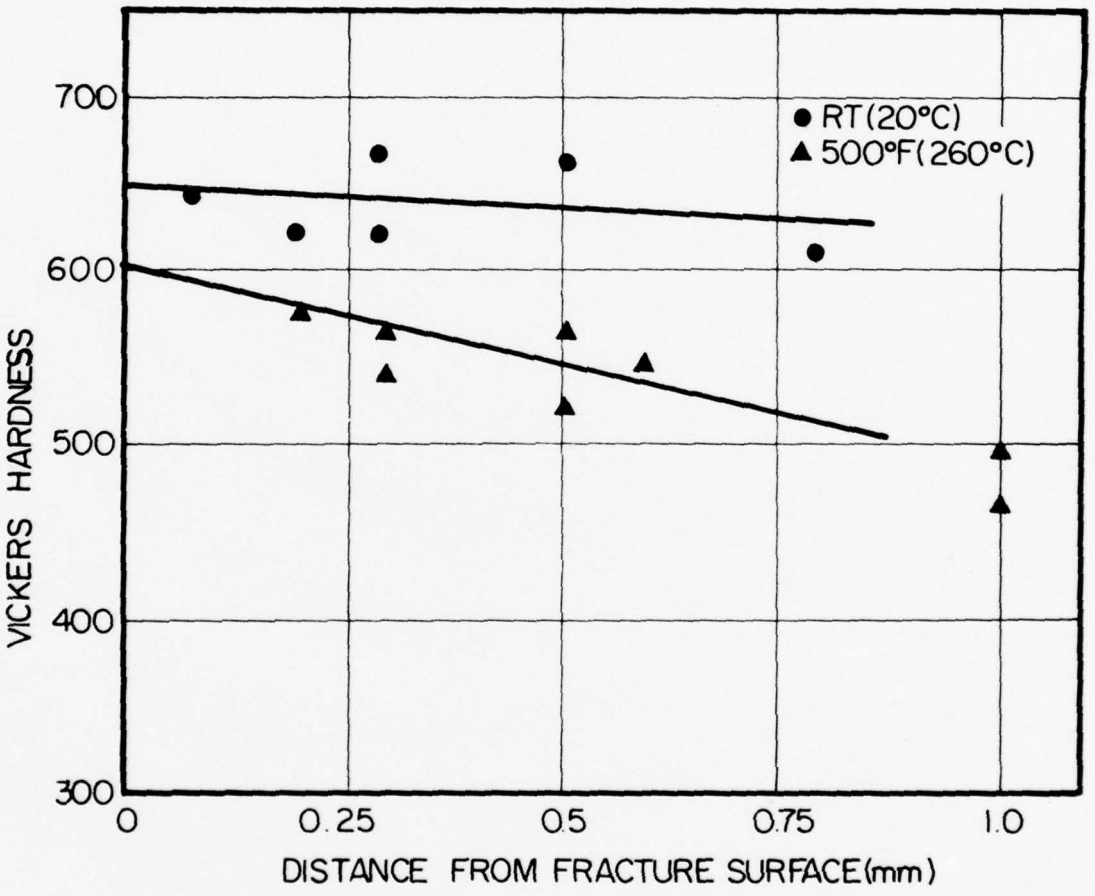

FIG. 5. VICKERS HARDNESS OF TRIP STEEL WIRE VS. DISTANCE FROM THE FRACTURE SURFACE FOR SPECIMENS TESTED AT ROOM TEMPERATURE AND 500°F (260°C).

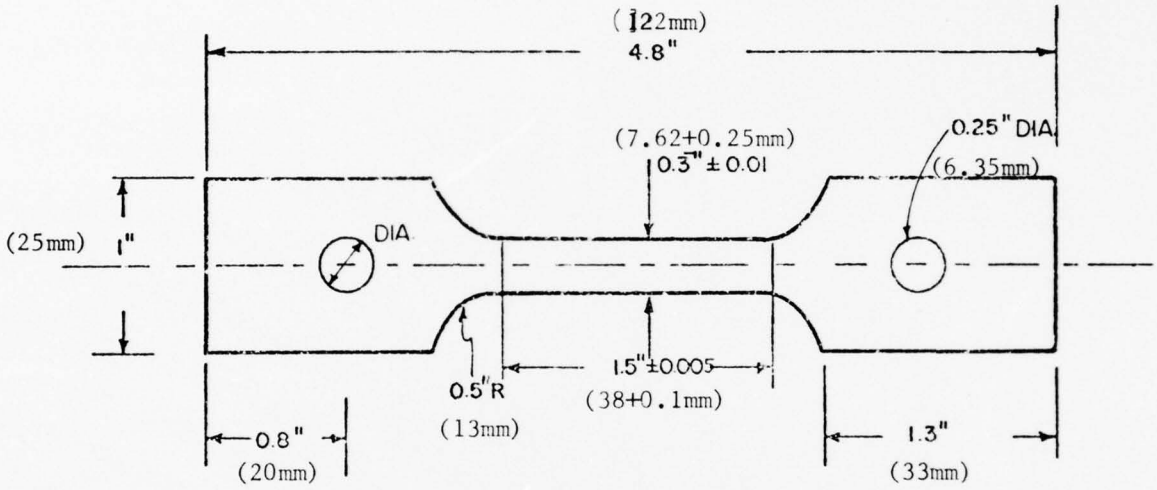

FIG. 6. TENSILE TEST SPECIMEN CONFIGURATION, AM 355 STAINLESS STEEL.

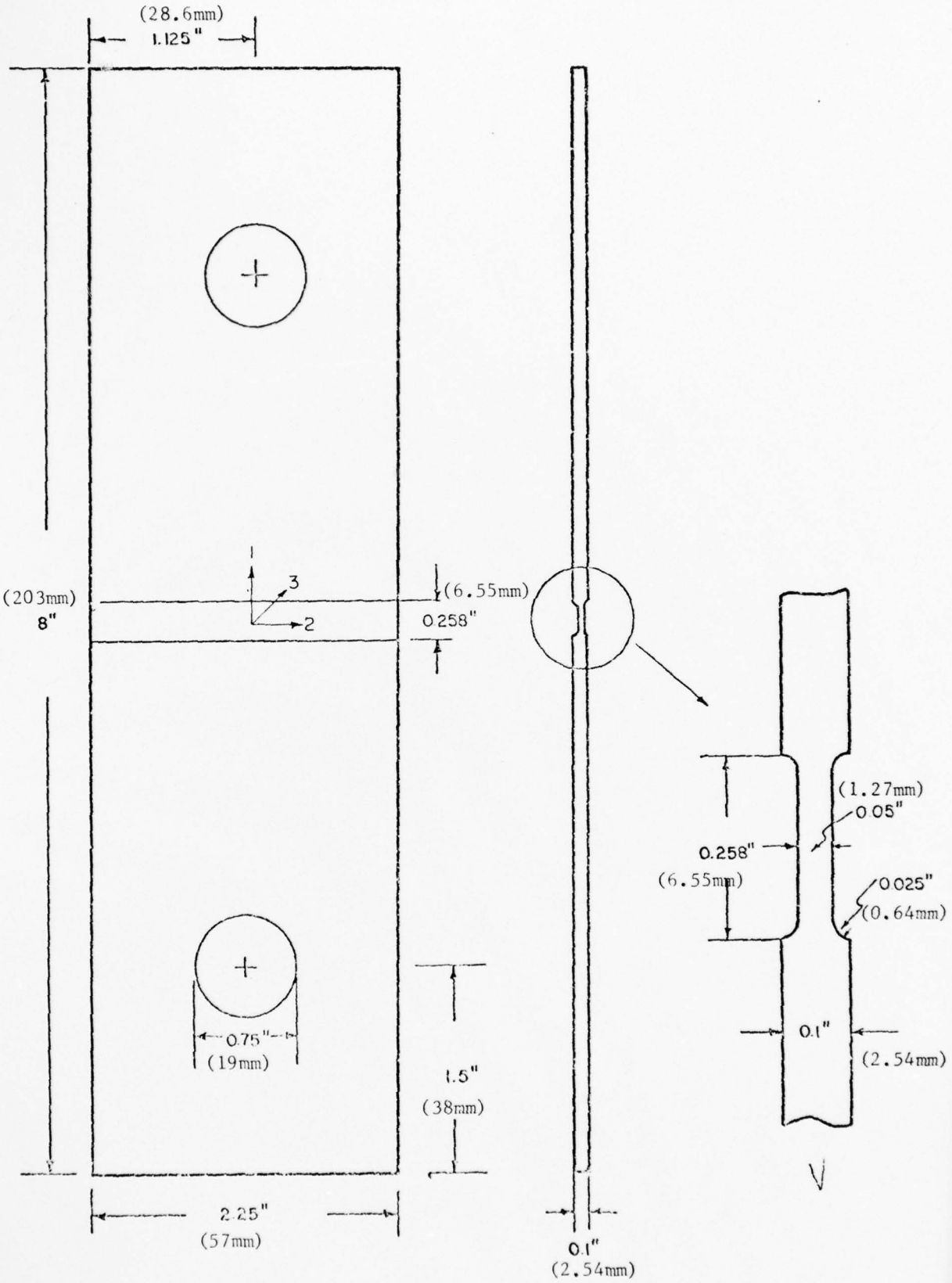

FIG. 7. PLANE STRAIN TENSION SPECIMEN.

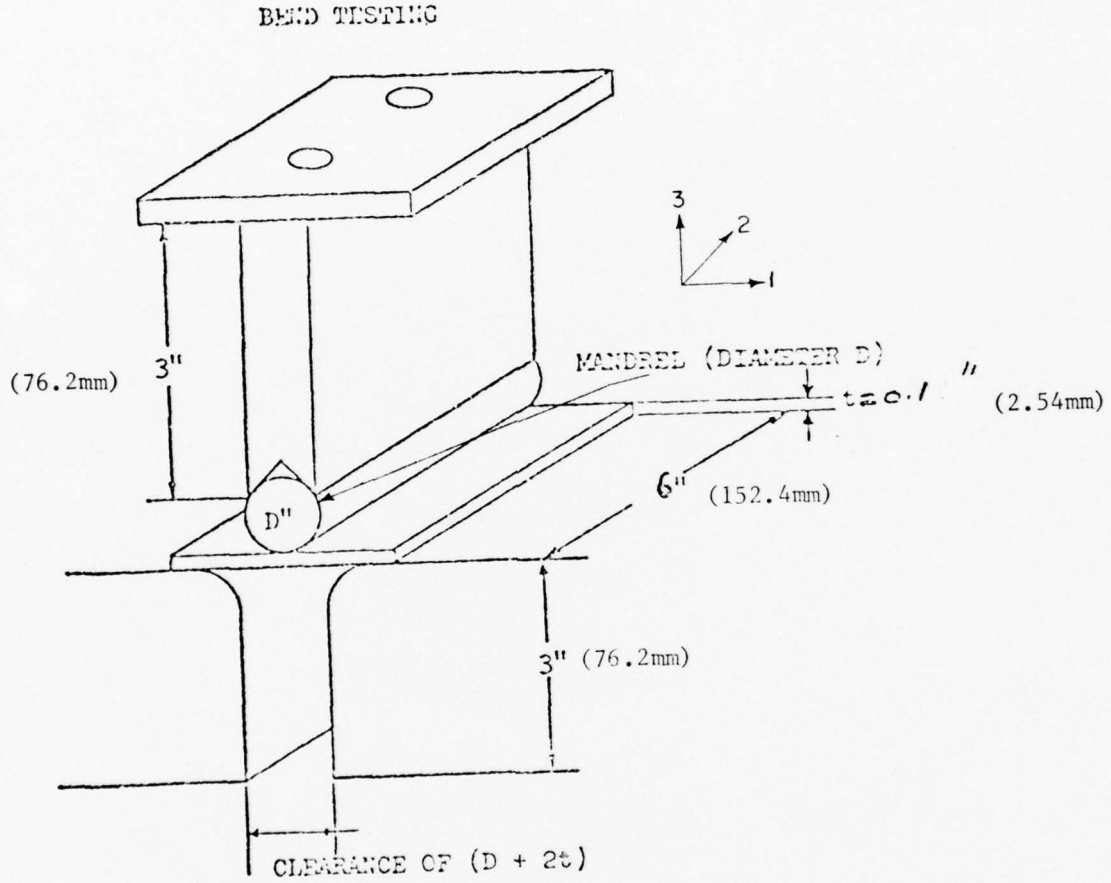

FIG. 8. EXPERIMENTAL SET-UP FOR PLANE STRAIN DUCTILITY TEST 2:1 BIAXIAL LOADING.

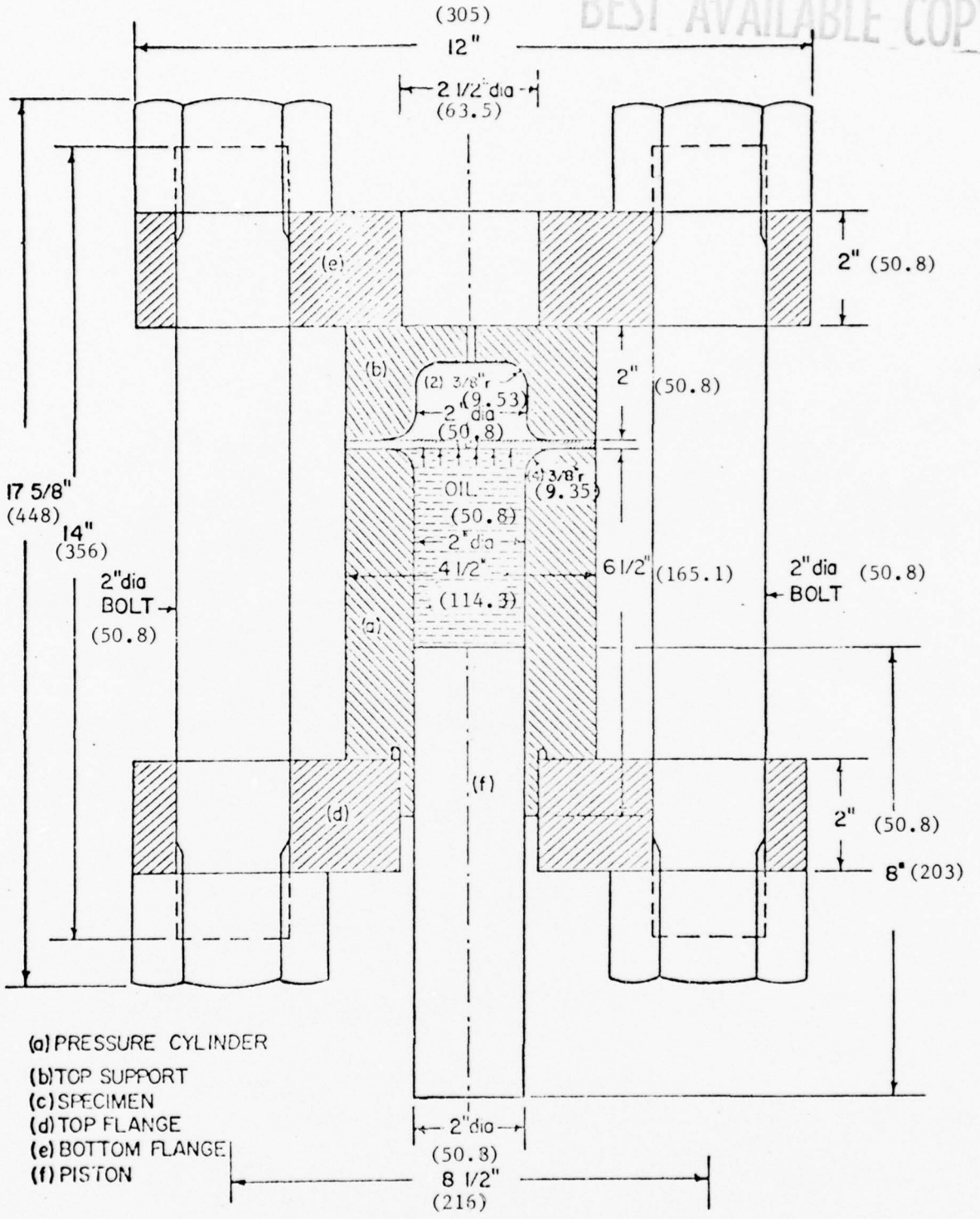

FIG. 9. HYDRAULIC BULGE FIXTURE FOR BALANCED BIAXIAL ($\sigma_2/\sigma_1 = 1$, $\sigma_3/\sigma_1 = 0$) TENSION TEST. DIMENSIONS IN () ARE IN mm.

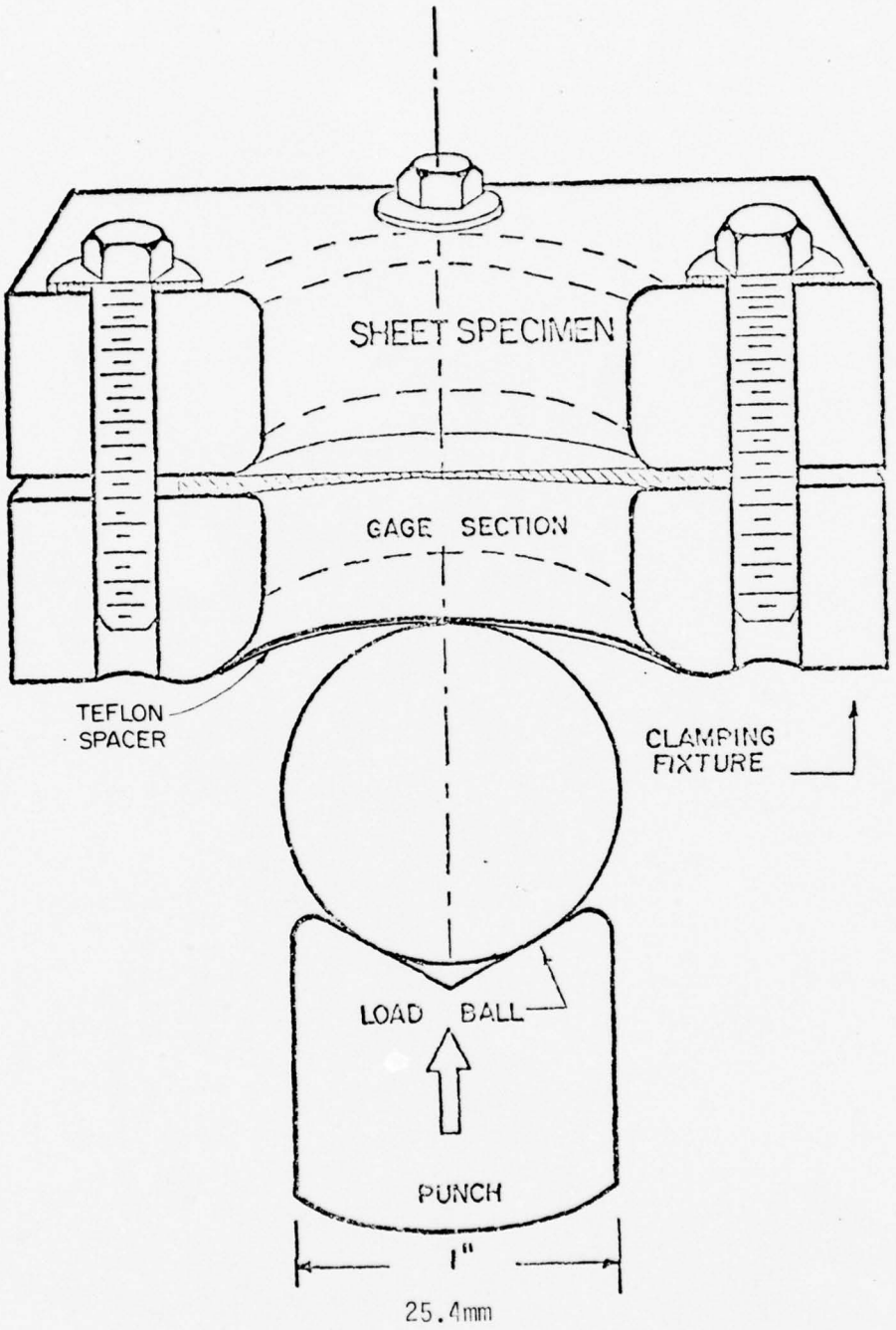

FIG. 10. SECTION VIEW OF THE MODIFIED AZRIN-BACKOFEN TESTING APPARATUS.

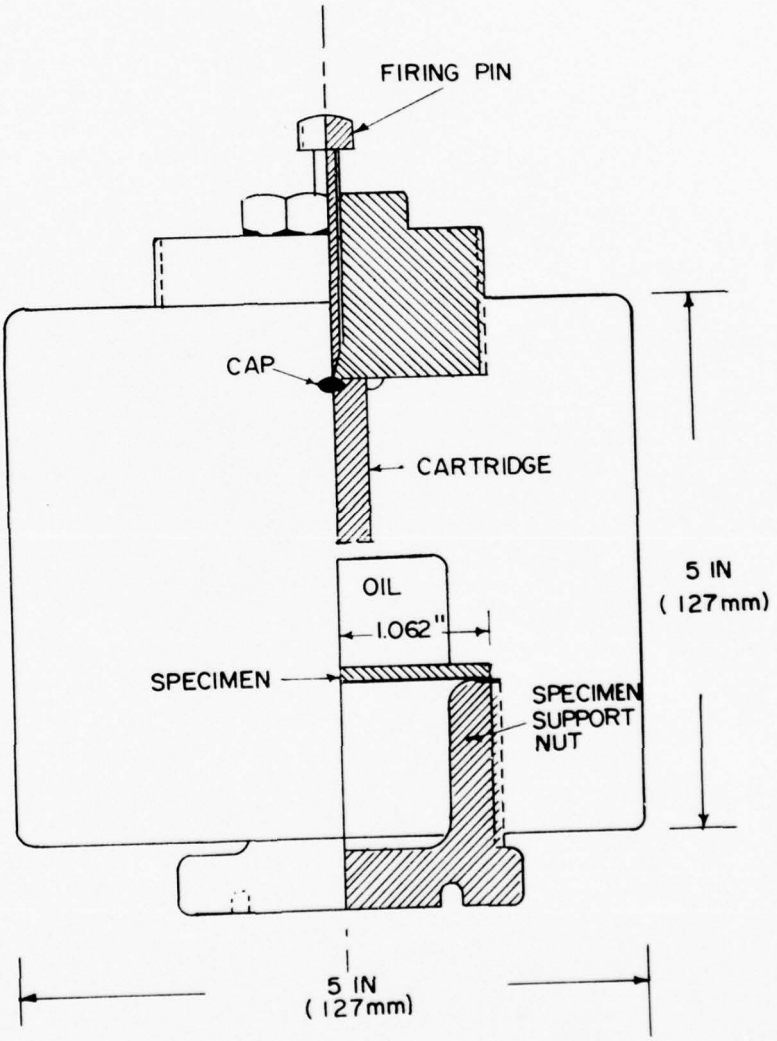

FIGURE 11 EXPLOSIVE BULGE TEST APPARATUS.

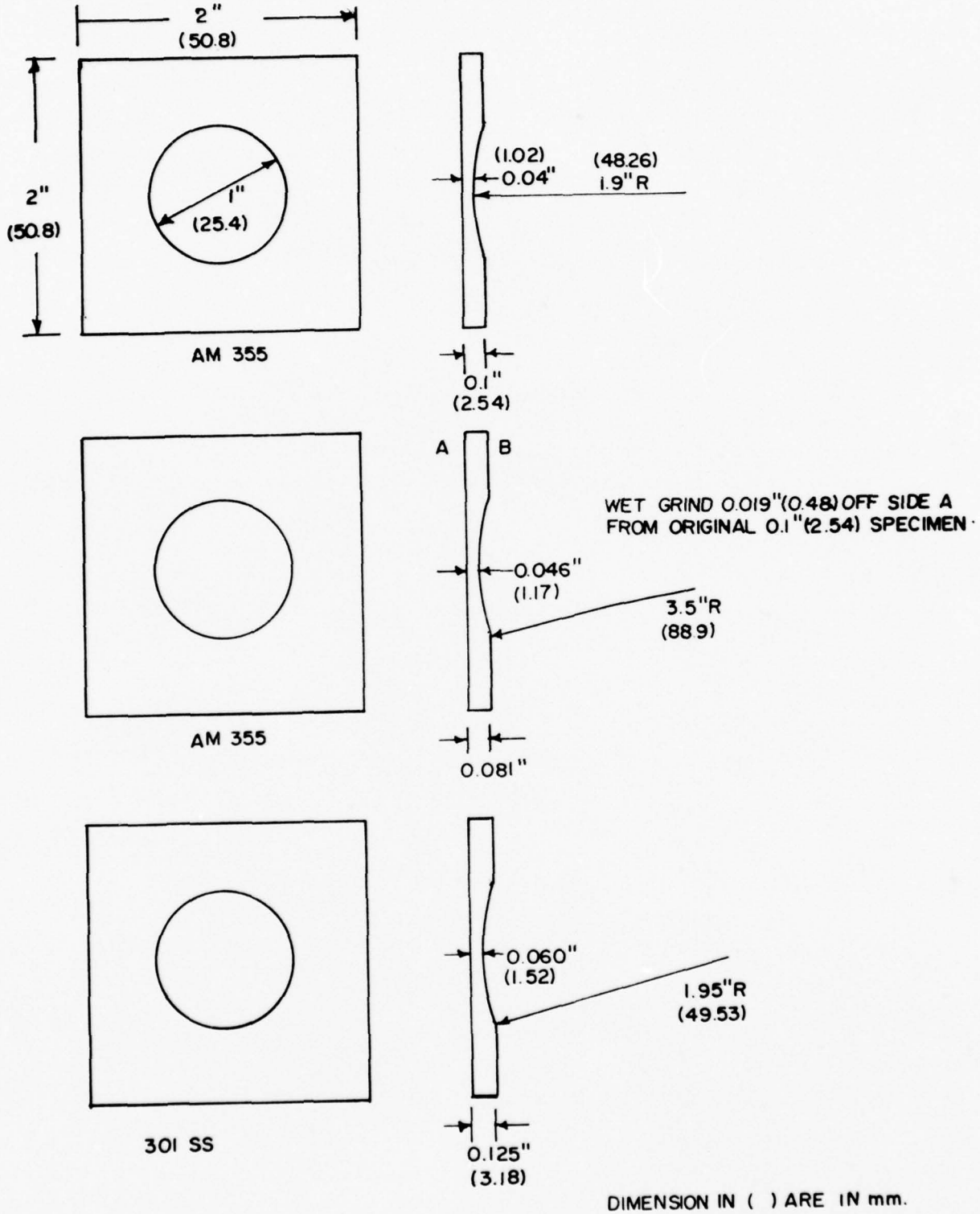

FIGURE I2. MINIATURE BULGE TEST SPECIMENS.

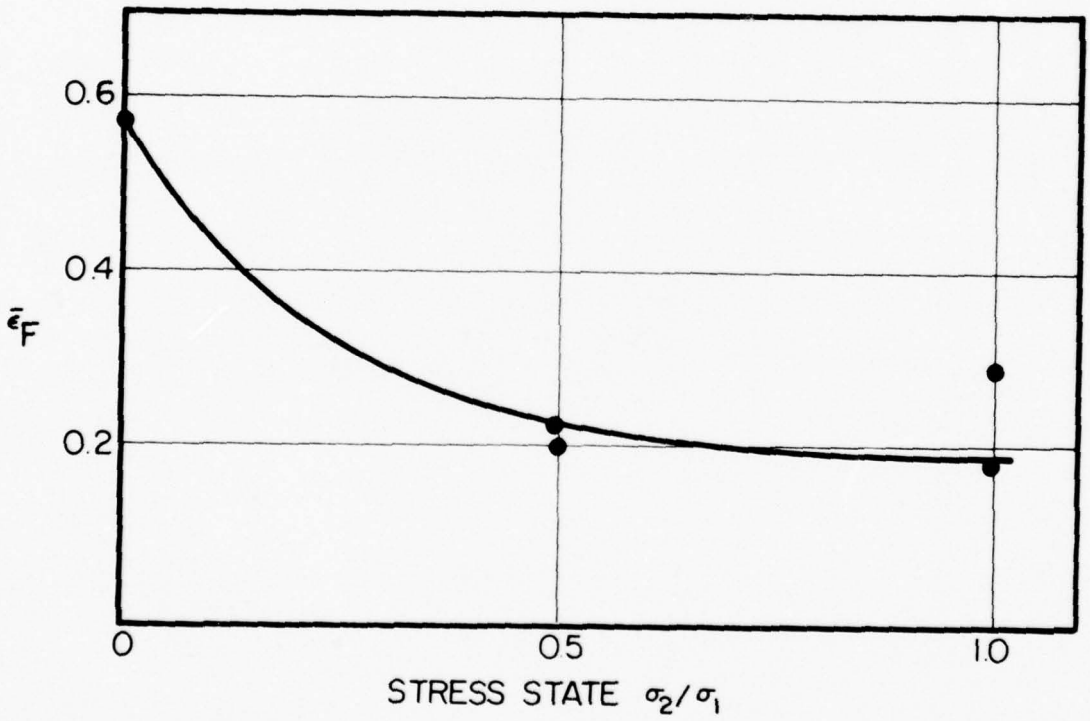

FIG. 13. EFFECT OF STRESS STATE ON EFFECTIVE FRACTURE DUCTILITY OF AM-355 CRT STEEL.

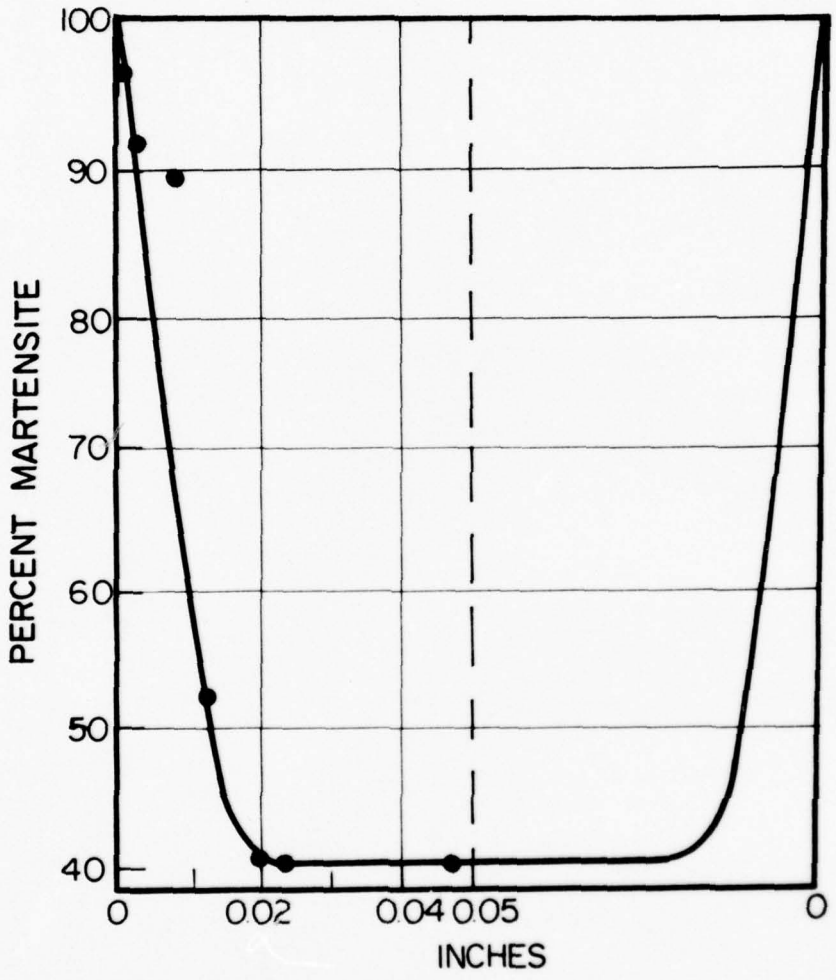

FIG. 14. THE VARIATION OF MARTENSITE THROUGH THICKNESS OF AM-355 CRT STEEL, MEASURED BY X-RAY DIFFRACTION.

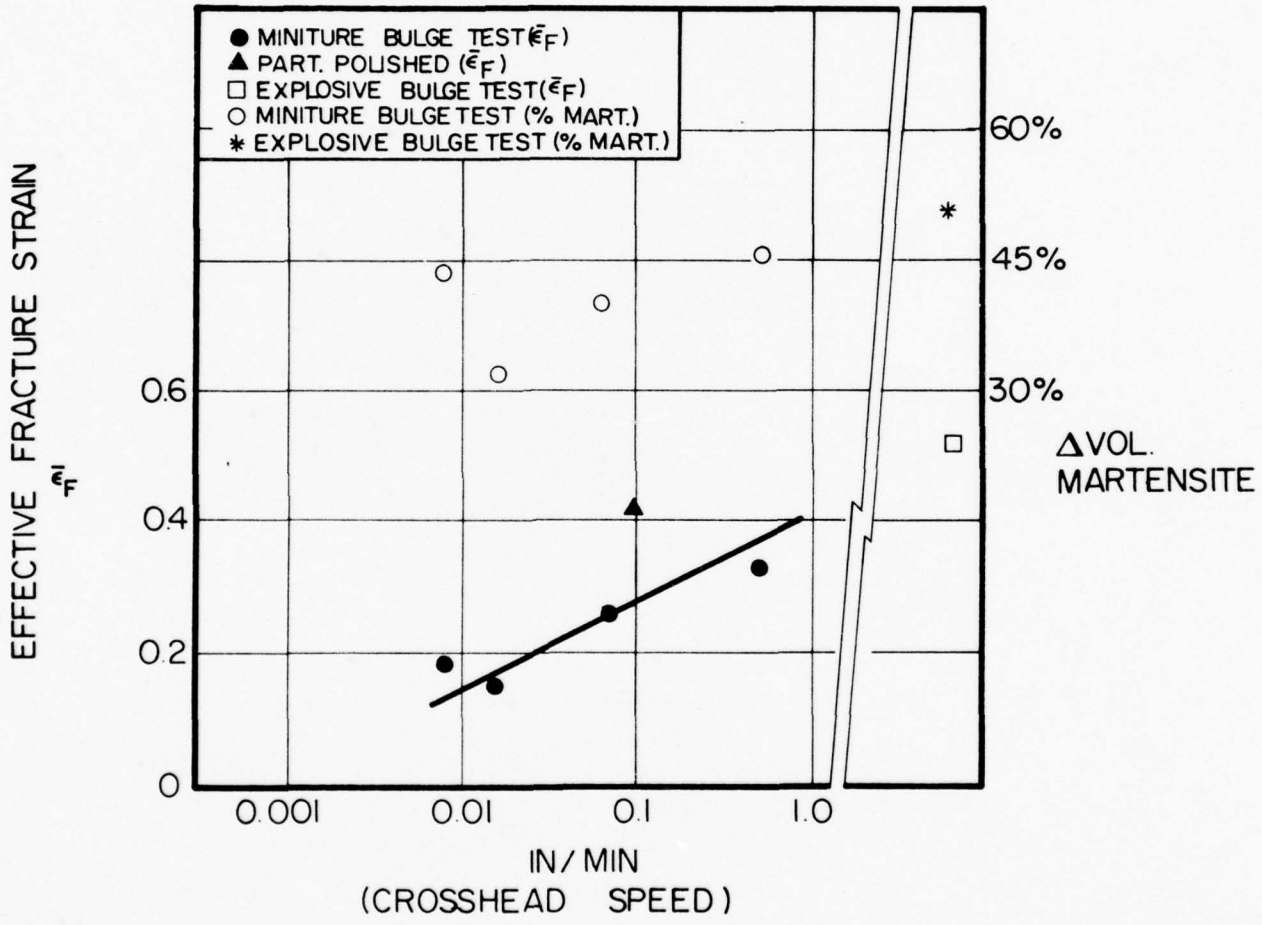

FIGURE 15. EFFECT OF CROSSHEAD SPEED ON BULGE DUCTILITY AND MARTENSITE FORMATION OF AM-355 CRT STEEL SHEET.

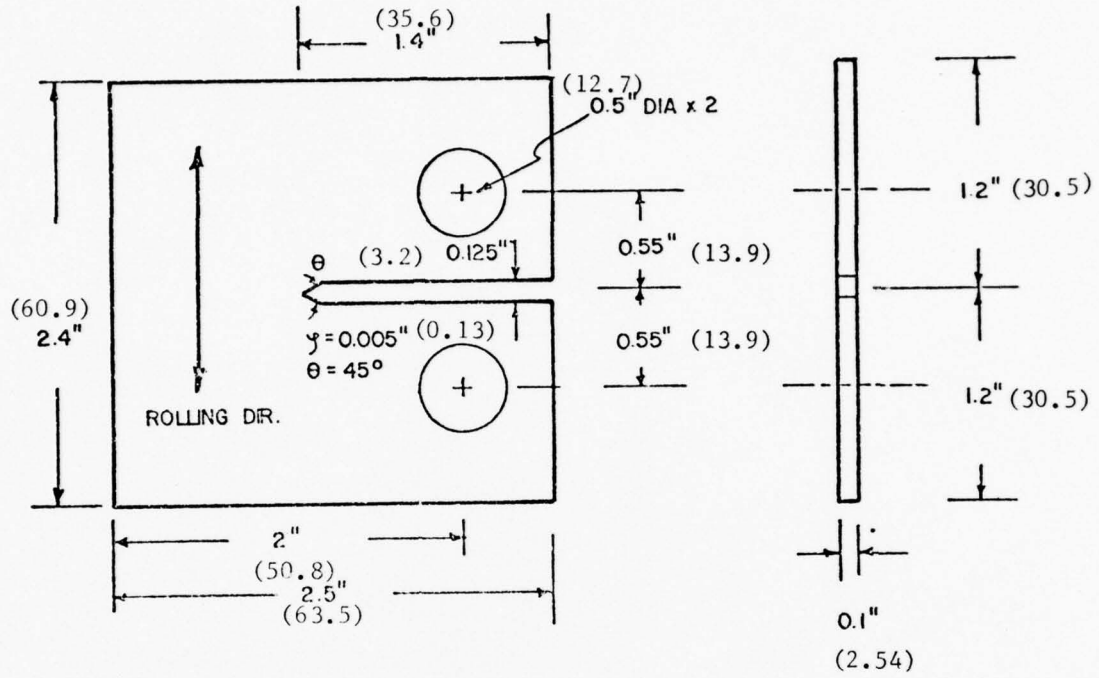

FIG. 16. SPECIMEN FOR FRACTURE TOUGHNESS TESTS. DIMENSIONS IN () ARE IN mm.

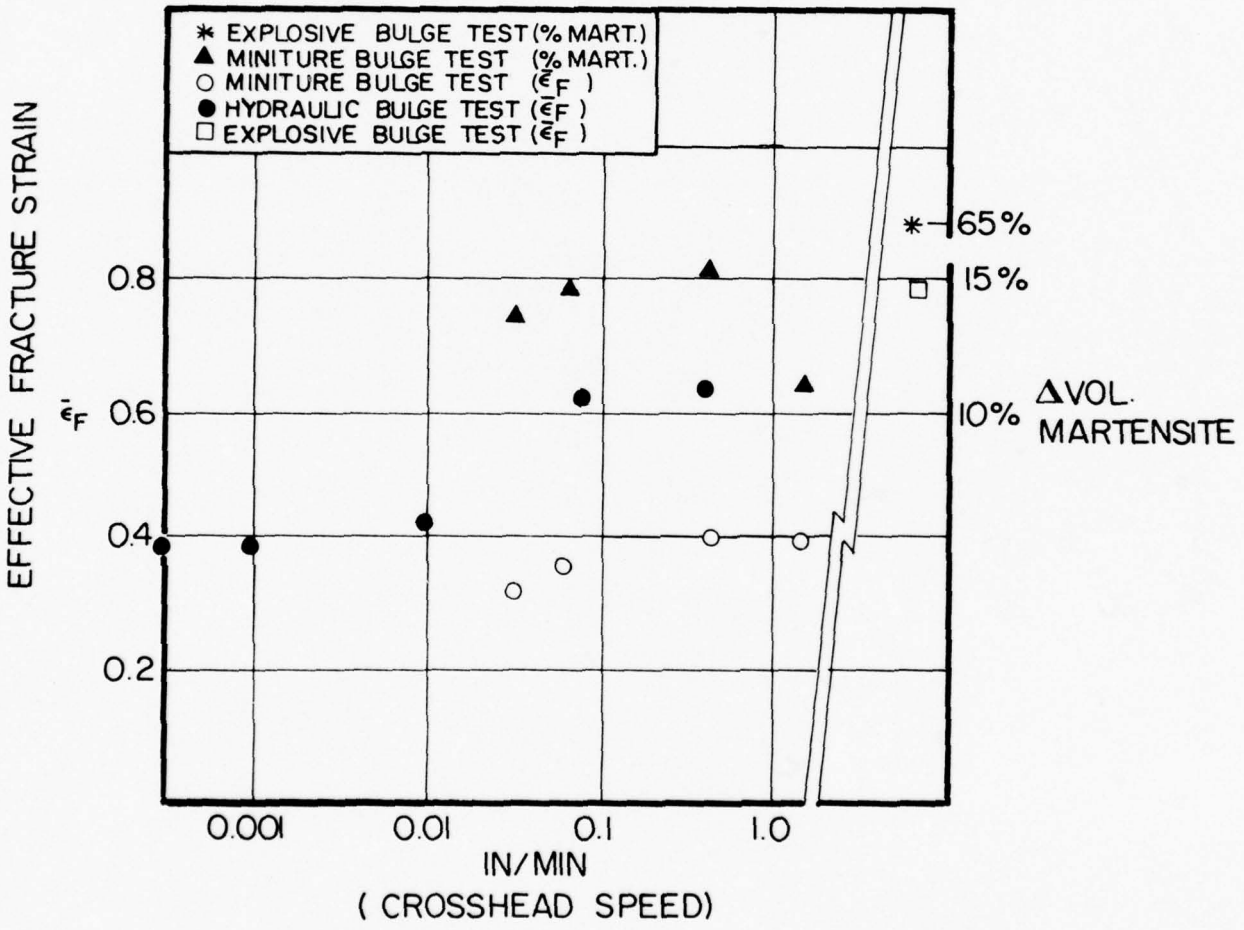

FIGURE 17. EFFECT OF CROSSHEAD SPEED ON BULGE DUCTILITY AND MARTENSITE FORMATION OF TYPE 301 STAINLESS STEEL.

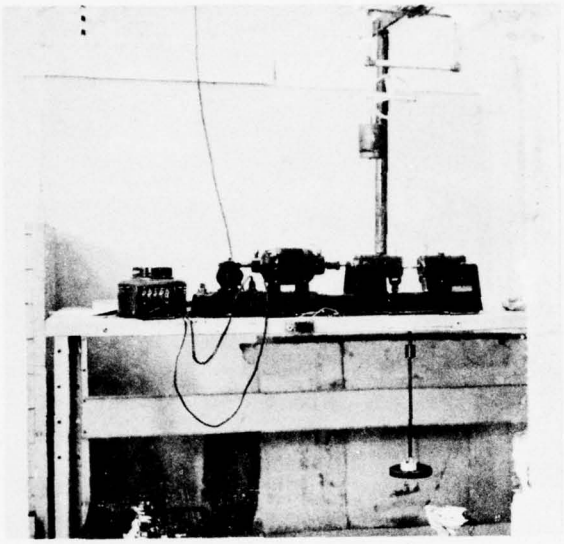

FIG.18 FATIGUE TESTING SYSTEM

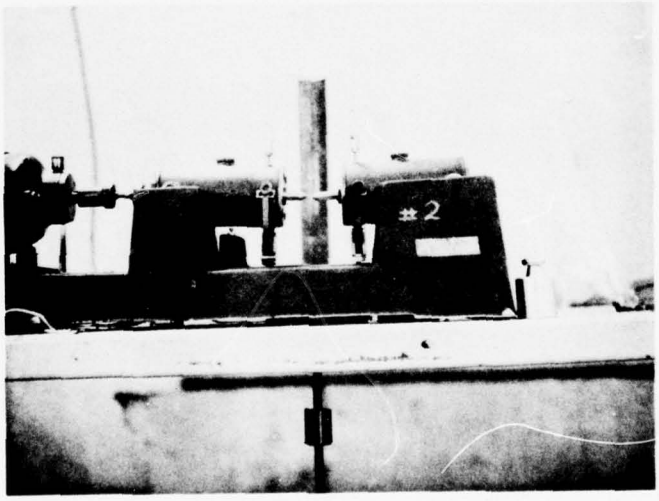

FIG.19 PIN VISES IN FATIGUE TESTING SYSTEM

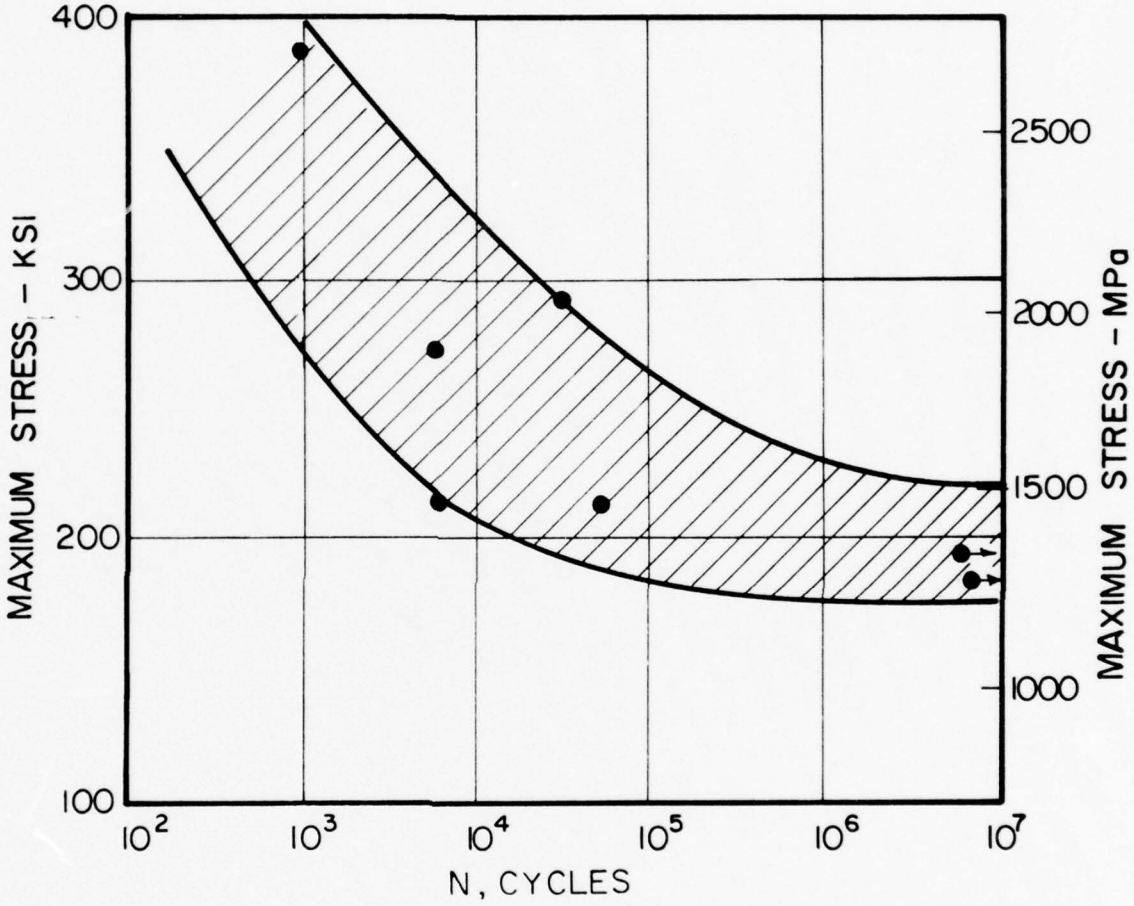

FIG. 20. ROTATIONAL BEAM S-N CURVE OF TRIP STEEL WIRE.

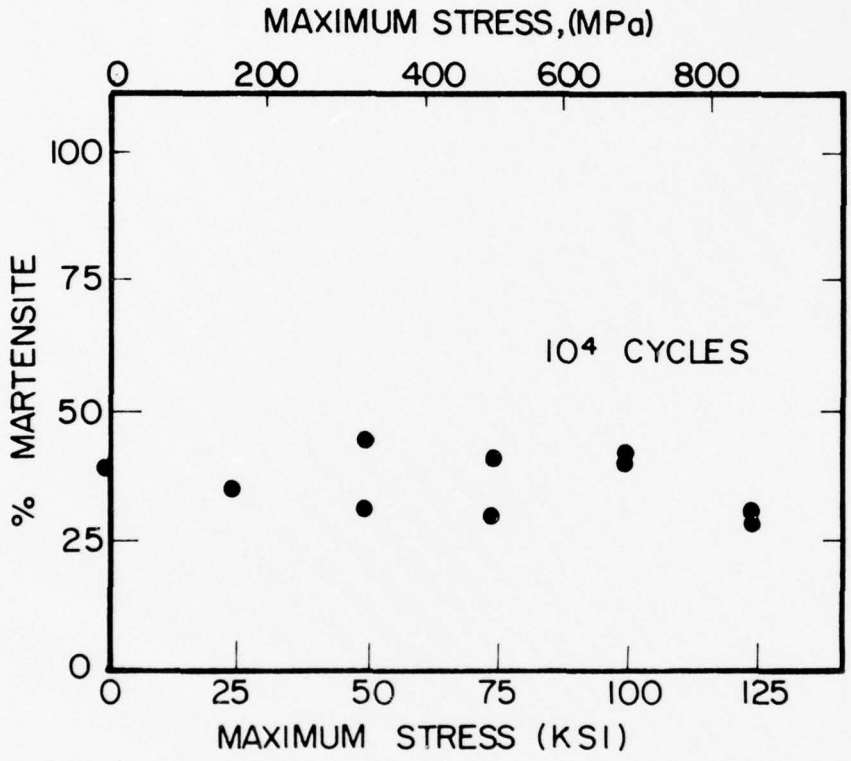

FIG. 21. MARTENSITE CONTENT OF TRIP STEEL WIRE AFTER 10,000 CYCLES TO THE MAXIMUM STRESS INDICATED. CYCLING IN TENSION-TENSION, R = 0.1.

TABLE I

CHEMICAL COMPOSITION OF TEST MATERIALS (WEIGHT PERCENT)

	TRIP Steel	AM-355 CRT[15]		Type 301 SS[16]	
		Min	Max	Min	Max
Carbon	0.20	0.10	0.15	---	0.15
Chromium	15.0	15.00	16.00	16.00	18.00
Cobalt	13.35				
Manganese	0.50	0.50	1.25	---	2.00
Molybdenum	5.10				
Nickel	1.50	4.00	5.00	6.00	8.00
Nitrogen	0.03	0.07	0.13		
Phosphorus	0.018		0.04	---	0.045
Silicon	0.13		0.50	---	1.00
Sulfur	0.028		0.030	---	0.030
Vanadium	0.17				
Iron		Balance			

AM-355 CRT MECHANICAL PROPERTIES FROM ALLEGHENY LUDLUM

Hardness R_c	Yield Strength .02%,psi (MPa)	Yield Strength .2%,psi (MPa)	Ultimate Strength psi (MPa)	Percent Elongation in 2 inch	$E \times 10^{-6}$ psi (MPa)
47.0	95,600 (658)	171,600 (1186)	217,000 (1496)	19.5	32.3 (0.22)
	101,100 (696)	176,700 (1120)	218,200 (1504)	19.5	30.5 (0.21)

TABLE II

TRIP STEEL TENSION TEST RESULTS

Original diameter	0.056 inch	1.42 mm
Original gage length	10.00 inch	254 mm
Final diameter	0.0405 inch	1.03 mm
Final gage length	10.718 inch	272.2 mm
Percent elongation	7.18 %	
Percent reduction in area	47.7 %	
Maximum load	745 lb	3310 N
Tensile strength	302 ksi	208 Nmm^{-2}
$\varepsilon_F = \ln A/A_f$	0.32	

Test was conducted at room temperature with crosshead approximately 0.1 inch/minute (2.5 mm/minute)

TABLE III

TENSILE TEST RESULTS OF AM-355 CRT STEEL SHEET

	Transverse Direction #1	Transverse Direction #2	Longitude Direction #1	Longitude Direction #2
Original cross-section area(A) (in^2)	(0.0294)	(0.0306)	(0.0305)	(0.0308)
(mm^2)	[19.00]	[19.7]	[19.7]	[19.9]
Fracture cross-section area(A_F) (in^2)	(0.0142)	(0.0160)	(0.0177)	(0.0189)
(mm^2)	[9.54]	[10.3]	[11.6]	[12.2]
Total elongation in 1.5 in: (in)	(0.295)	(0.270)	(0.350)	(0.340)
38 mm: [mm]	[7.49]	[6.86]	[8.89]	[8.64]
Maximum load (lb)	(6,520)	(6.760)	(6,800)	(6,740)
[N]	[29,000]	[30,100]	[30,200]	[30,000]
Fracture load (lb)	(5,700)	(6,000)	(5,940)	(5,960)
[N]	[25,300]	[26,700]	[26,400]	[26,500]
Yield strength 0.2% (ksi)	(171.8)	(171.6)	(180.3)	(179.9)
[MPa]	[1180]	[1180]	[1240]	[1240]
Tensile strength (ksi)	(221.4)	(220.9)	(194.4)	(218.8)
[MPa]	[1530]	[1520]	[1340]	[1510]
Elastic modulus ($\times 10^6$ psi)	(28.0)	(27.4)	(27.9)	(27.4)
[GPa]	[193]	[189]	[192]	[189]
Fracture strain $\varepsilon_F = \ln (A/A_F)$	0.69	0.65	0.54	0.49

TABLE IV

MINIATURE BULGE TEST RESULTS OF AM-355 CRT STEEL SHEET

Specimen	Initial Thickness, t_i [in] (mm)	Fracture Thickness, t_f [in] (mm)	Martensite Content* Before Bulge Test (%)	Martensite Content* After Bulge Test (%)	$\bar{\varepsilon}_F = -\ln \frac{t_f}{t_i}$	Comment
#1	[0.039] (0.99)	[0.0365] (0.93)		96		Some minor cracks appear at rims
#2	[0.0443] (1.135)	[0.030] (0.76)	94	96	0.39	
#3	[0.050] (1.27)	[0.0365] (0.93)	96	97	0.31	Large cracks appear at rims
#4	[0.0395] (1.00)	[0.0295] (0.75)			0.29	

* Martensite content was obtained on the surface and thus is not representative of the bulk

TABLE V

MINIATURE BULGE TEST RESULTS OF AM-355 CRT SHEET
FOR VARIOUS CROSSHEAD SPEEDS

	Initial Thickness t_i (in) [mm]	Fracture Thickness t_f (in) [mm]	Volume Percent Martensite* Before Test	Volume Percent Martensite* After Test	Crosshead Speed (in/mm)	Maximum Load (lb) [N]	$\bar{\varepsilon}_F = -\ln \frac{t_f}{t_i}$	Δ Martensite* Volume Percent
#1	(0.0403) [1.024]	(0.034) [0.864]	41	85	0.009	(12,100) [53,800]	0.17	43
#2	(0.0393) [9.998]	(0.0336) [0.853]	55	88	0.0155	(12,500) [55,600]	0.157	33
#3	(0.0436) [1.109]	(0.0336) [0.853]	52	94	0.08	(15,600) [69,400]	0.26	41
#4	(0.0404) [1.026]	(0.0291) [0.739]	46 46	91 91	0.6	(16,200) [72,000]	0.328	45
#5	(0.043) [1.092]	(0.0283) [0.719]	84	97	0.1	(18,000) [80,000]	0.418	13

* Martensite content depends on amount of surface removal

TABLE VI

EXPLOSIVE BULGE TEST RESULTS FOR AM-355 CRT AND 301 SS

	Initial Thickness (in) [mm]	Fracture Thickness (in) [mm]	Volume Percent Martensite*		Δ Martensite Percent	$\bar{\varepsilon}_F$	Comment **
			Before Test	After Test			
AM-355							
#1	(0.0402) [1.021]	Did not break	44	--	--	--	4 tries
#2	(0.0347) [0.88]	(0.021) [0.53]	32	83	50	0.51	2 tries
301 SS							
#1	(0.0256) [0.65]	Did not break	21	--	--	--	2 tries
#2	(0.0256) [0.65]	(0.0118) [0.30]	22	88	66	0.77	1 try
#3	(0.0257) [0.65]	(0.0117) [0.30]	28	92	64	0.79	2 tries
#4	(0.0256) [0.65]	(0.0120) [0.30]	33	96	63	0.76	3 tries

* Martensite content depends on amount of surface removal

**The explosive bulge test was conducted with a powder charge. If the amount of powder was insufficient to cause fracture, the test was repeated on the same specimen; e.g. 1 try means that the specimen broke on the first attempt, etc.

TABLE VII

FRACTURE TOUGHNESS TEST RESULTS FOR AM-355 CRT

Specimen #	Volume Percent Martensite		Thickness t	Width w	Crack Length	$\frac{a}{w}$	$f(\frac{a}{w})$	P_Q	K_Q	Comment
	Before Test	After Test	(in) [mm]	(in) [mm]	(in) [mm]			(lb) [N]	(ksi$\sqrt{in}$)	
1	79	88	(0.102) [2.59]	(2.0) [50.8]	(1.00) [25.4]	0.50	9.60	(1,950) [8,690]	129.9	This specimen subjected to anti-plane force
2	95	96	(0.1025) [2.60]	(2.0) [50.8]	(0.912) [53.2]	0.456	8.46	(1,870) [8,340]	109.4	
3	58	81	(0.063) [1.60]	(1.97) [50.1]	(0.976) [24.8]	0.495	9.46	(950) [4,220]	101.9	Wet ground

TABLE VIII

HYDRAULIC BULGE TEST RESULTS FOR HALF HARD 301 SS

	Initial Thickness t_i (in) [mm]	Fracture Thickness t_f (in) [mm]	Volume Percent Martensite		Crosshead Speed (in/min)	Maximum Load (lb) [N]	$\bar{\varepsilon}_F$
			Before Test	After Test			
#1	(0.0253) [0.643]	(0.0170) [0.432]	27	99	0.001	(22,000) [97,900]	0.40
#2	(0.0256) [0.656]	(0.0165) [0.419]	--	99	0.01	(20,700) [92,100]	0.43
#3	(0.0256) [0.650]	(0.014) [0.355]	--	99	0.08	---	0.61
#4	(0.0257) [0.653]	(0.0139) [0.353]	--	99	0.3	(22,500) [100,100]	0.61

TABLE IX

MINIATURE BULGE TEST RESULTS FOR FULLY HARDENED 301 SS

	Initial Thickness (in) [mm]	Final Thickness (in) [mm]	Volume Percent Martensite		Crosshead Speed (in/min)	Maximum Load (lb) [N]	ε_F	Δ Martensite Volume Percent
			Before Test	After Test				
#1	(0.058) [1.48]	(0.043) [1.07]	84	97	0.027	(22,800) [101,000]	0.33	13
#2	(0.0601) [1.526]	(0.0411) [1.04]	84	99	0.06	(25,800) [115,000]	0.38	14
#3	(0.0612) [1.544]	(0.0406) [1.031]	83	98	0.5	(25,000) [111,000]	0.41	15
#4	(0.0619) [1.57]	(0.0413) [1.05]	84	95	1.5	(24,300) [108,100]	0.40	11

REFERENCES

1. Zackay, V. F., Parker, E. R., Fahr, D. and Busch, R., "The Enchancement of Ductility in High Strength Steels", Trans., ASM Vol. 60, p. 252 (June 1967).

2. Weiss, V., "Transformation Plasticity", ASM Pre-Congress Seminar on the Inhomogeneity of Plastic Deformation, Detroit (Oct. 1971).

3. Weiss. V., Schroder, K., Sanford, W., Chandan, H., Kunio, T., Lal, D. and Sengupta, M., "The Relationships Between the Transformation Characteristics and the Fracture and Fatigue Properties of TRIP Steels", Final Report AMMRC CTR 73-50 (December 1973).

4. Azrin, M., Olson, G. B. and Gagne, R. A., "Inhomogenous Deformation and Strain-Rate Effects in High-Stength TRIP Steels", AMMRC TR 73-12 (March 1973).

5. Private Communication, Morris Azrin, AMMRC (1976).

6. Foner, S., "Versatile and Sensitive Vibrating-Sample Magnetometer", The Review of Scientific Instruments, Vol. 30, p. 548 (July 1956).

7. "Standard Method of Tests for Vickers Hardness of Metallic Materials", 1972 Annual Book of ASTM Standards, p. 364, ASTM Designation E92-72 (1972).

8. Corrigan, D. A., Travis, R. E., Ardito, V. P. and Adams, Jr., C. M., "Bi-Axial Strength of Welds in Heat-Treated Sheet Steel", Welding Journal, Vol. 4, p. 123S-128S (March 1962).

9. Clausing, D. P., "Effect of Plastic Strain State on Ductility and Toughness", Int. J. of Fracture Mech., Vol. 6, p. 71 (1970).

10. Azrin, M. and Backofen, W. A., "The Deformation and Failure of a Biaxially Stretched Sheet", Met. Trans., Vol. 1, p. 2857 (Oct. 1970).

11. Private Communication, J. E. Biegel (1975).

12. "Standard Method of Test for Plane Strain Fracture Toughness of Metallic Materials", 1973 Annual Book of ASTM Standards, Part 31, p. 960, ASTM Designation E399-73 (1973).

13. Weiss, V., Kasai, Y. and Sieradzki, K. in Properties Related to Fracture Toughness, ASTM STP 605, American Society for Testing and Materials, 1976, p. 16-33.

14. Weiss, V., Kasai, Y. and Sieradzki, K., "Microstructural Aspects of Fracture Toughness", Symposium on Properties Related to Fracture Toughness, Montreal, Canada, June 26, 1975.

15. Weiss, V. and Sessler, J. G. (editors), "Aerospace Structural Metals Handbook", Vo. 1, Code 1505, Syracuse University Press (1967).

16. Weiss, V. and Sessler, J. G. (editors), "Aerospace Structural Metals Handbook", Vol. 1, Code 1301, Syracuse University Press (1967).

APPENDIX

Processing of TRIP Steel

One 3000-lb induction heat was melted for supplying this material. The chemical composition of the heat is as follows:

C	Mn	P	S	Si	Ni	Cr	V
0.20	0.50	0.018	0.028	0.13	1.50	15.0	0.17

Mo	Co	N
5.10	13.35	0.03

The heat was cast in 14-inch ingots.

Forging of Ingots

The 14-inch square ingots were heated to 2100°F and forged to 13-inch square billets. These billets were then ground to remove all surface defects.

Rolling of Billets

The 13-inch billets were heated to 2100°F and rolled to 3-1/4 inch square billets. These billets were ground to remove the decarburized layer and surface defects.

Rolling and Annealing of Rods

The 3-1/4 inch square billets were rolled to 0.250-inch diameter rods using the heating process used for making billets. The 0.250-inch rods were solution treated at 2100°F and water quenched. The rods were then pickled to remove scale and graphite coated for hot drawing.

Processing of 0.056- and 0.054-inch Diameter Wire

The 0.250-inch rod was warm drawn to 0.150-inch diameter in 5 equal reductions and then austenitized at 200°F and water quenched. The austenitized wire was pickled and coated with graphite. The wire was then warm drawn at 800°F to 0.060-inch diameter for the making of 0.056-inch diameter wire and to 0.058 for drawing to 0.054-inches. This drawing was done in 8 equal passes. The 0.056-inch diameter wire was cold drawn from 0.060-inch diameter. The 0.054-inch diameter wire was cold drawn from 0.058-inch diameter.

The tensile properties of the 0.056-inch and the 0.054-inch diameter wire are given as follows:

Wire Diameter	Yield Strength	Tensile Strength	Elongation
0.056-inches	300,000 psi	337,000 psi	17%
0.054-inches	301,000 psi	333,000 psi	18%

Processing of 0.041-inch Diameter Wire

The 0.250-inch diameter rod was warm drawn 0.115-inches in 7 equal reductions and then austenitized at 2000°F and water quenched. The austenitized wire was pickled and coated with graphite. This wire was then warm drawn at 800°F to 0.044-inch diameter. The 0.044-inch wire was then cold drawn to 0.041-inches. The tensile properties of the 0.041-inch wire are given below:

Wire Diameter	Yield Strength	Tensile Strength	Elongation
0.041-inches	304,000 psi	334,000 psi	16%

EFFECT OF STRAIN RATE ON THE PROPERTIES OF TRIP STEEL

	Test Speed (in/min)	Tensile Strength (psi)	Elongation in 10 inch gage Percent
0.056 inch Diameter	.05	308,400	19.4
	.10	304,700	21.9
	.56	282,000	12.5
	1.00	292,200	5.0
0.054 inch Diameter	.05	329,500	19.1
	.10	325,400	16.9
	.56	296,800	13.8
	1.00	310,000	10.7
0.041 inch Diameter	.05	310,700	18.5
	.10	291,800	15.6
	.56	293,900	11.3
	1.00	--*	--*

*Specimen broke in grips

Syracuse University
Department of Chemical Engineering and
Materials Science
Syracuse, New York 13210

Ad

UNCLASSIFIED
UNLIMITED DISTRIBUTION

THE RELATIONSHIPS BETWEEN THE TRANSFORMATION CHARACTERISTICS AND THE FRACTURE AND FATIGUE PROPERTIES OF TRIP STEELS AND OTHER METASTABLE AUSTENITIC STEELS

Key Words

V. Weiss, K. Schroder, P. Sherman and A. Pan,
Syracuse University, Syracuse, N.Y. 13210

TRIP steels
High strength steels
Stainless steels
Fracture toughness

Transformation plasticity
Phase transformation
Mechanical Properties
Fatigue Properties

Final Report AMMRC CTR 77-1, January 1977, 49 pp.
illus - tables, Contract DAAG46-75-C-0065 D/A Proj:
1T162105AH84, AMCMS Code: 612105.11.148400 Final Report
March 19, 1975 to July 18, 1976

Transformation plasticity was studied in TRIP steel wire, AM-355 CRT stainless steel sheet and two grades of type 301 stainless steel sheet. In the partially cold worked TRIP steel wire (yield strength 2070 MPa, tensile strength 2325 MPa) transformation plasticity is manifested by a martensite increase from 2% to 95% at fracture (ε_f=0.32, σ_f=4000 MPa) at room temperature. The first stage of martensite formation occurs during plastic straining to 0.04-0.1 when the martensite increases from 2% to 70%. Further straining to fracture, within less than two wire diameters gage length, causes further transformation to nearly 100% martensite. The rotating beam fatigue endurance limit (1350 MPa) is higher than anticipated from the tensile strength, probably due to a significant amount of martensite formation in the failure zone. No martensite is formed for tension-tension cycling for 10,000 cycles and maximum stresses up to 862 MPa. For AM-355 CRT the fracture ductility decreases with increasing stress biaxiality from 0.6 for uniaxial tension to 0.2 for plane strain tension and bulge tests. In the bulge test the martensite content increases from 45 to 85% for a strain of 0.2. Increasing the strain rate causes an increase in the bulge ductility to 0.5 for explosive tests ($\dot{\varepsilon} \sim 10^3$ sec^{-1}). The plane stress fracture toughness for AM-355 CRT was measured as approximately 100 MNm$^{-3/2}$ with the formation of approximately 20% martensite near the crack zone. Type 301 stainless steel (half hard grade) also showed significant increase in bulge ductility with increasing strain rate from 0.4 under quasi static loading to 0.8 under explosive ($\dot{\varepsilon} \sim 10^3$ sec^{-1}) with a concomitant martensite transformation from approximately 20% to over 90%.

Syracuse University
Department of Chemical Engineering and
Materials Science
Syracuse, New York 13210

Ad

UNCLASSIFIED
UNLIMITED DISTRIBUTION

THE RELATIONSHIPS BETWEEN THE TRANSFORMATION CHARACTERISTICS AND THE FRACTURE AND FATIGUE PROPERTIES OF TRIP STEELS AND OTHER METASTABLE AUSTENITIC STEELS

Key Words

V. Weiss, K. Schroder, P. Sherman and A. Pan,
Syracuse University, Syracuse, N.Y. 13210

TRIP steels
High strength steels
Stainless steels
Fracture toughness

Transformation plasticity
Phase transformation
Mechanical Properties
Fatigue Properties

Final Report AMMRC CTR 77-1, January 1977, 49 pp.
illus - tables, Contract DAAG46-75-C-0065 D/A Proj:
1T162105AH84, AMCMS Code: 612105.11.148400 Final Report
March 19, 1975 to July 18, 1976

Transformation plasticity was studied in TRIP steel wire, AM-355 CRT stainless steel sheet and two grades of type 301 stainless steel sheet. In the partially cold worked TRIP steel wire (yield strength 2070 MPa, tensile strength 2325 MPa) transformation plasticity is manifested by a martensite increase from 2% to 95% at fracture (ε_f=0.32, σ_f=4000 MPa) at room temperature. The first stage of martensite formation occurs during plastic straining to 0.04-0.1 when the martensite increases from 2% to 70%. Further straining to fracture, within less than two wire diameters gage length, causes further transformation to nearly 100% martensite. The rotating beam fatigue endurance limit (1350 MPa) is higher than anticipated from the tensile strength, probably due to a significant amount of martensite formation in the failure zone. No martensite is formed for tension-tension cycling for 10,000 cycles and maximum stresses up to 862 MPa. For AM-355 CRT the fracture ductility decreases with increasing stress biaxiality from 0.6 for uniaxial tension to 0.2 for plane strain tension and bulge tests. In the bulge test the martensite content increases from 45 to 85% for a strain of 0.2. Increasing the strain rate causes an increase in the bulge ductility to 0.5 for explosive tests ($\dot{\varepsilon} \sim 10^3$ sec^{-1}). The plane stress fracture toughness for AM-355 CRT was measured as approximately 100 MNm$^{-3/2}$ with the formation of approximately 20% martensite near the crack zone. Type 301 stainless steel (half hard grade) also showed significant increase in bulge ductility with increasing strain rate from 0.4 under quasi static loading to 0.8 under explosive ($\dot{\varepsilon} \sim 10^3$ sec^{-1}) with a concomitant martensite transformation from approximately 20% to over 90%.

Syracuse University
Department of Chemical Engineering and
Materials Science
Syracuse, New York 13210

Ad

UNCLASSIFIED
UNLIMITED DISTRIBUTION

THE RELATIONSHIPS BETWEEN THE TRANSFORMATION CHARACTERISTICS AND THE FRACTURE AND FATIGUE PROPERTIES OF TRIP STEELS AND OTHER METASTABLE AUSTENITIC STEELS

Key Words

V. Weiss, K. Schroder, P. Sherman and A. Pan,
Syracuse University, Syracuse, N.Y. 13210

TRIP steels
High strength steels
Stainless steels
Fracture toughness

Transformation plasticity
Phase transformation
Mechanical Properties
Fatigue Properties

Final Report AMMRC CTR 77-1, January 1977, 49 pp.
illus - tables, Contract DAAG46-75-C-0065 D/A Proj:
1T162105AH84, AMCMS Code: 612105.11.148400 Final Report
March 19, 1975 to July 18, 1976

Transformation plasticity was studied in TRIP steel wire, AM-355 CRT stainless steel sheet and two grades of type 301 stainless steel sheet. In the partially cold worked TRIP steel wire (yield strength 2070 MPa, tensile strength 2325 MPa) transformation plasticity is manifested by a martensite increase from 2% to 95% at fracture (ε_f=0.32, σ_f=4000 MPa) at room temperature. The first stage of martensite formation occurs during plastic straining to 0.04-0.1 when the martensite increases from 2% to 70%. Further straining to fracture, within less than two wire diameters gage length, causes further transformation to nearly 100% martensite. The rotating beam fatigue endurance limit (1350 MPa) is higher than anticipated from the tensile strength, probably due to a significant amount of martensite formation in the failure zone. No martensite is formed for tension-tension cycling for 10,000 cycles and maximum stresses up to 862 MPa. For AM-355 CRT the fracture ductility decreases with increasing stress biaxiality from 0.6 for uniaxial tension to 0.2 for plane strain tension and bulge tests. In the bulge test the martensite content increases from 45 to 85% for a strain of 0.2. Increasing the strain rate causes an increase in the bulge ductility to 0.5 for explosive tests ($\dot{\varepsilon} \sim 10^3$ sec^{-1}). The plane stress fracture toughness for AM-355 CRT was measured as approximately 100 MNm$^{-3/2}$ with the formation of approximately 20% martensite near the crack zone. Type 301 stainless steel (half hard grade) also showed significant increase in bulge ductility with increasing strain rate from 0.4 under quasi static loading to 0.8 under explosive ($\dot{\varepsilon} \sim 10^3$ sec^{-1}) with a concomitant martensite transformation from approximately 20% to over 90%.

DISTRIBUTION LIST

No. of Copies	To
1	Office of the Director, Defense Research and Engineering, The Pentagon, Washington, D. C. 20301
12	Commander, Defense Documentation Center, Cameron Station, Building 5, 5010 Duke Street, Alexandria, Virginia 22314
1	Metals and Ceramics Information Center, Battelle Columbus Laboratories, 505 King Avenue, Columbus, Ohio 43201
	Chief of Research and Development, Department of the Army, Washington, D. C. 20310
2	ATTN: Physical and Engineering Sciences Division
	Commander, Army Research Office, P. O. Box 12211, Research Triangle Park, North Carolina 27709
1	ATTN: Information Processing Office
	Commander, U. S. Army Materiel Development and Readiness Command, 5001 Eisenhower Avenue, Alexandria, Virginia 22333
1	ATTN: DRCLDC, Mr. R. Zentner
1	DRCSA-S, Dr. R. B. Dillaway, Chief Scientist
	Commander, U. S. Army Electronics Command, Fort Monmouth, New Jersey 07703
1	ATTN: DRSEL-GG-DD
1	DRSEL-GG-DM
1	DRSEL-GG-E
1	DRSEL-GG-EA
1	DRSEL-GG-ES
1	DRSEL-GG-EG
	Commander, U. S. Army Missile Command, Redstone Arsenal, Alabama 35809
1	ATTN: Technical Library
1	DRSMI-RSM, Mr. E. J. Wheelahan
	Commander, U. S. Army Armament Command, Rock Island, Illinois 61201
2	ATTN: Technical Library
1	DRSAR-SC, Dr. C. M. Hudson
1	DRSAR-PPW-PB, Mr. Francis X. Walter
	Commander, U. S. Army Natick Research and Development Command, Natick, Massachusetts 01760
1	ATTN: Technical Library
1	Dr. E. W. Ross
1	DRXNM-AAP, Mr. J. Falcone
	Commander, U. S. Army Satellite Communications Agency, Fort Monmouth, New Jersey 07703
1	ATTN: Technical Document Center

No. of Copies	To
	Commander, U. S. Army Tank-Automctive Research and Development Command, Warren, Michigan 48090
1	ATTN: DRDTA-R
2	DRDTA, Research Library Branch
	Commander, White Sands Missile Range, New Mexico 88002
1	ATTN: STEWS-WS-VT
	Commander, Aberdeen Proving Ground, Maryland 21005
1	ATTN: STEAP-TL, Bldg. 305
	Commander, Edgewood Arsenal, Aberdeen Proving Ground, Maryland 21010
1	ATTN: Mr. F. E. Thompson, Dir. of Eng. & Ind. Serv., Chem-Mun Br
	Commander, Frankford Arsenal, Philadelphia, Pennsylvania 19137
1	ATTN: Library, H1300, Bl. 51-2
1	SARFA-L300, Mr. J. Corrie
	Commander, U. S. Army Ballistic Research Laboratory, Aberdeen Proving Ground, Maryland 21005
1	ATTN: Dr. J. Frasier
1	Dr. R. Vitali
1	Dr. G. L. Filbey
1	Dr. R. Karpp
1	Dr. W. Gillich
	Commander, Harry Diamond Laboratories, 2800 Powder Mill Road, Adelphi, Maryland 20783
1	ATTN: Technical Information Office
	Commander, Picatinny Arsenal, Dover, New Jersey 07801
1	ATTN: SARPA-RT-S
1	SARPA-FR-M-D, PLASTEC, A. M. Anzalone
1	Mr. A. Devine
	Commander, Redstone Scientific Information Center, U. S. Army Missile Command, Redstone Arsenal, Alabama 35809
4	ATTN: DRSMI-RBLD, Document Section
	Commander, Watervliet Arsenal, Watervliet, New York 12189
1	ATTN: SARWV-RDT, Technical Information Services Office
1	Dr. T. Davidson
1	Mr. D. P. Kendall
1	Mr. J. F. Throop
1	SARWV-RDR, Dr. F. W. Schmiedeshoff
	Commander, U. S. Army Foreign Science and Technology Center, 220 7th Street, N. E., Charlottesville, Virginia 22901
1	ATTN: DRXST-SD2

No. of Copies	To
	Commander, U. S. Army Aeromedical Research Unit, P. O. Box 577, Fort Rucker, Alabama 36460
1	ATTN: Technical Library
	Director, Eustis Directorate, U. S. Army Air Mobility Research and Development Laboratory, Fort Eustis, Virginia 23604
1	ATTN: Mr. J. Robinson, SAVDL-EU-SS
1	Mr. R. Berresford
	Librarian, U. S. Army Aviation School Library, Fort Rucker, Alabama 36360
1	ATTN: Building 5907
	Commander, U. S. Army Agency for Aviation Safety, Fort Rucker, Alabama 36362
1	ATTN: Librarian, Building 4905
	Commander, USACDC Air Defense Agency, Fort Bliss, Texas 79916
1	ATTN: Technical Library
	Commander, U. S. Army Engineer School, Fort Belvoir, Virginia 22060
1	ATTN: Library
	Commander, U. S. Army Engineer Waterways Experiment Station, Vicksburg, Mississippi 39180
1	ATTN: Research Center Library
	Aeronautic Structures Laboratories, Naval Air Engineering Center, Philadelphia, Pennsylvania 19112
1	ATTN: Library
	Naval Air Development Center, Aero Materials Department, Warminster, Pennsylvania 18974
1	ATTN: J. Viglione
	Naval Ship Research and Development Laboratory, Annapolis, Maryland 21402
1	ATTN: Dr. H. P. Chu
	Naval Underwater Systems Center, New London, Connecticut 06320
1	ATTN: R. Kasper
	Naval Research Laboratory, Washington, D. C. 20375
1	ATTN: Dr. J. M. Krafft - Code 8430
2	Dr. G. R. Yoder - Code 6382
1	C. D. Beachem
	Chief of Naval Research, Arlington, Virginia 22217
1	ATTN: Code 471

No. of Copies	To
	Naval Weapons Laboratory, Washington, D. C. 20390
1	ATTN: H. W. Romine
	Director, Structural Mechanics Research, Office of Naval Research, 800 North Quincy Street, Arlington, Virginia 22203
1	ATTN: Dr. N. Perrone
1	Ship Structure Committee, Maritime Transportation Research Board, National Research Council, 2101 Constitution Avenue, N. W., Washington, D. C. 20418
	Air Force Materials Laboratory, Wright-Patterson Air Force Base, Ohio 45433
2	ATTN: AFML/MXE/E. Morrissey
1	AFML/LC
1	AFML/LLP/D. M. Forney, Jr.
1	AFML/MBC/Mr. Stanley Schulman
1	AFML/LNC/T. J. Reinhart
1	AFFDL (FB), Dr. J. C. Halpin
1	Dr. S. Tsai
1	Dr. N. Pagano
	Air Force Flight Dynamics Laboratory, Wright-Patterson Air Force Base, Ohio 45433
1	ATTN: AFFDL (FBC), C. Wallace
1	AFFDL (FBCB), G. D. Sendeckyj
	National Aeronautics and Space Administration, Washington, D. C. 20546
1	ATTN: Mr. B. G. Achhammer
1	Mr. G. C. Deutsch - Code RR-1
	National Aeronautics and Space Administration, Marshall Space Flight Center, Huntsville, Alabama 35812
1	ATTN: R-P&VE-M, R. J. Schwinghamer
1	S&E-ME-MM, Mr. W. A. Wilson, Building 4720
	National Aeronautics and Space Administration, Langley Research Center, Hampton, Virginia 23365
1	ATTN: Mr. H. F. Hardrath, Mail Stop 129
1	Mr. R. Foye, Mail Stop 188A
	National Aeronautics and Space Administration, Lewis Research Center, 21000 Brook Park Road, Cleveland, Ohio 44135
1	ATTN: Mr. S. S. Manson
1	Dr. J. E. Srawley, Mail Stop 105-1
1	Mr. W. F. Brown, Jr.
	Panametrics, 221 Crescent Street, Waltham, Massachusetts 02154
1	ATTN: Mr. K. A. Fowler

No. of Copies	To
	Wyman-Gordon Company, Worcester, Massachusetts 01601
1	ATTN: Technical Library
	Lockheed-Georgia Company, Marietta, Georgia 30063
1	ATTN: Advanced Composites Information Center, Dept. 72-34 - Zone 26
	National Bureau of Standards, U. S. Department of Commerce, Washington, D. C. 20234
1	ATTN: Mr. J. A. Bennett
1	Mr. W. F. Anderson, Atomics International, Canoga Park, California 91303
	Midwest Research Institute, 425 Coker Boulevard, Kansas City, Missouri 64110
1	ATTN: Mr. C. Q. Bowles
1	Mr. J. C. Grosskreutz
1	Mr. A. Hurlich, General Dynamics Convair, Mail Zone 572-00, P. O. Box 1128, San Diego, California 92112
	Virginia Polytechnic Institute and State University, Dept. of Engineering Mechanics, 230 Norris Hall, Blacksburg, Virginia 24061
1	ATTN: Prof. R. M. Barker
1	Assoc. Prof. G. W. Swift
	Southwest Research Institute, 8500 Culebra Road, San Antonio, Texas 78284
1	ATTN: Mr. G. C. Grimes
	IIT Research Institute, Chicago, Illinois 60616
1	ATTN: Dr. I. M. Daniel
1	Dr. R. E. Johnson, Mgr., Mechanics of Materials-AEG, Mail Drop M88, General Electric Company, Cincinnati, Ohio 45215
1	Mr. J. G. Kaufman, Alcoa Research Laboratories, New Kensington, Pennsylvania 15068
1	Mr. G. M. Orner, MANLABS, 21 Erie Street, Cambridge, Massachusetts 02139
1	Mr. P. N. Randall, TRW Systems Group - 0-1/2210, One Space Park, Redondo Beach, California 90278
	TRW Equipment, TRW Inc., 23555 Euclid Avenue, Cleveland, Ohio 44117
1	ATTN: Dr. E. A. Steigerwald, T/M-3296
1	Dr. I. S. Tuba, Basic Technology, Inc., 7125 Saltsburg Road, Pittsburgh, Pennsylvania 15235
1	Mr. B. M. Wundt, 2346 Shirl Lane, Schenectady, New York 12309

No. of Copies	To
1	Mr. W. A. Van der Sluys, Research Center, Babcock and Wilcox, Alliance, Ohio 44601
	Battelle Columbus Laboratories, 505 King Avenue, Columbus, Ohio 43201
1	ATTN: Dr. E. Rybicki
1	Dr. K. R. Merckx, Battelle Northwest Institute, Richland, Washington 99352
	General Electric Company, Schenectady, New York 12010
1	ATTN: Mr. A. J. Brothers, Materials and Processes Laboratory
	General Electric Company, Knolls Atomic Power Laboratory, P. O. Box 1072, Schenectady, New York 12301
1	ATTN: Mr. F. J. Mehringer
1	Mr. L. F. Coffin, General Electric Research Laboratory, P. O. Box 1088, Schenectady, New York 12301
	United States Steel Corporation, Monroeville, Pennsylvania 15146
1	ATTN: Dr. A. K. Shoemaker, Applied Research Laboratory
	Westinghouse Electric Company, Pittsburgh, Pennsylvania 15235
1	ATTN: Mr. R. E. Peterson, Research Laboratories
1	Mr. E. T. Wessel, Research and Development Center
1	Mr. B. F. Langer, Westinghouse Nuclear Energy Systems, P. O. Box 355, Pittsburgh, Pennsylvania 15230
1	Mr. M. J. Manjoine, Westinghouse Research Laboratory, Churchill Boro, Pittsburgh, Pennsylvania 15235
	Brown University, Providence, Rhode Island 02912
1	ATTN: Prof. J. R. Rice
1	Prof. W. N. Findley, Division of Engineering, Box D
	Carnegie-Mellon University, Department of Mechanical Engineering, Schenley Park, Pittsburgh, Pennsylvania 15213
1	ATTN: Dr. J. L. Swedlow
1	Prof. J. Dvorak, Chemical Engineering Department, Duke University, Durham, North Carolina 27706
	Westinghouse Electric Company, Bettis Atomic Power Laboratory, P. O. Box 109, West Mifflin, Pennsylvania 15122
1	ATTN: Mr. M. L. Parrish
	George Washington University, School of Engineering and Applied Sciences, Washington, D. C. 20006
1	ATTN: Dr. H. Liebowitz

No. of Copies	To
	Lehigh University, Bethlehem, Pennsylvania 18015
1	ATTN: Prof. George R. Irwin
1	Prof. G. C. Sih
1	Prof. F. Erodgan
	Massachusetts Institute of Technology, Cambridge, Massachusetts 02139
1	ATTN: Prof. T. H. H. Pian, Department of Aeronautics and Astronautics
1	Prof. F. J. McGarry
1	Prof. A. S. Argon, Room 1-312
1	Mr. William J. Walker, Air Force Office of Scientific Research, 1400 Wilson Boulevard, Arlington, Virginia 22209
1	Prof. R. Greif, Dept. of Mech. Eng., Tufts University, Medford, Massachusetts 02155
1	Dr. D. E. Johnson, AVCO Systems Division, Wilmington, Massachusetts 01887
1	Prof. B. Pipes, Dept. of Mech. Eng., Drexel University, Philadelphia, Pennsylvania 19104
1	Prof. A. Tetelman, Dept. of Materials Science, University of California, Los Angeles, California 90024
1	Prof. W. Goldsmith, Dept. of Mech. Eng., University of California, Berkeley, California 94700
1	Prof. A. J. McEvilly, University of Connecticut, Storrs, Connecticut 06268
1	Prof. D. Drucker, Dean of School of Engineering, University of Illinois, Champaign, Illinois 61820
	University of Illinois, Urbana, Illinois 61820
1	ATTN: Prof. H. T. Corten, Dept. of Theoretical and Applied Mechanics, 212 Talbot Laboratory
1	Dr. M. L. Williams, Dean of Engineering, 240 Benedum Hall, University of Pittsburgh, Pittsburgh, Pennsylvania 15261
1	Prof. A. Kobayashi, Dept. of Mechanical Engineering, University of Washington, Seattle, Washington 98105
1	Mr. W. A. Wood, Baillieu Laboratory, University of Melbourne, Melbourne, Australia
1	Mr. Elmer Wheeler, Airesearch Manufacturing Company, 402 S. 36th Street, Phoenix, Arizona 85034

No. of Copies	To
1	Mr. Charles D. Roach, U. S. Army Scientific and Technical Information Team, 6000 Frankfurt/Main, I. G. Hochhaus, Room 750, West Germany (APO 09710, NY)
1	Prof. R. Jones, Dept. of Civil Eng., Ohio State University, 206 W 18th Avenue, Columbus, Ohio 43210
	State University of New York at Stony Brook, Stony Brook, New York 11790
1	ATTN: Prof. Fu-Pen Chiang, Dept. of Mechanics
	E. I. Du Pont de Nemours and Company, Wilmington. Delaware 19898
1	ATTN: Dr. Carl Zweren, Industrial Fibers Division, Textile Fibers Dept.
	Washington University, St. Louis, Missouri 63130
1	ATTN: Prof. E. M. Wu
	General Dynamics, Convair Aerospace Division, P. O. Box 748, Fort Worth, Texas 76101
1	ATTN: Mfg. Engineering Technical Library
	Director, Army Materials and Mechanics Research Center, Watertown, Massachusetts 02172
2	ATTN: DRXMR-PL
1	DRXMR-PR
1	DRXMR-X
1	DRXMR-CT
1	DRXMR-AP

BEST AVAILABLE COPY

Syracuse University
Department of Chemical Engineering and
Materials Science
Syracuse, New York 13210

AD ______
UNCLASSIFIED
UNLIMITED DISTRIBUTION

THE RELATIONSHIPS BETWEEN THE TRANSFORMATION CHARACTERISTICS AND THE FRACTURE AND FATIGUE PROPERTIES OF TRIP STEELS AND OTHER METASTABLE AUSTENITIC STEELS
V. Weiss, K. Schroder, P. Sherman and A. Pan,
Syracuse University, Syracuse, N.Y. 13210
Final Report AMMRC CTR 77-1, January 1977, 49 pp.
illus - tables, Contract DAAG46-75-C-0065 D/A Proj:
1T162105AH84, AMCMS Code: 612105.11.148400 Final Report
March 19, 1975 to July 18, 1976.

Key Words

TRIP steels	Transformation plasticity
High strength steels	Phase transformation
Stainless steels	Mechanical Properties
Fracture toughness	Fatigue Properties

Transformation plasticity was studied in TRIP steel wire, AM-355 CRT stainless steel sheet and two grades of type 301 stainless steel sheet. In the partially cold worked TRIP steel wire (yield strength 2070 MPa, tensile strength 2325 MPa) transformation plasticity is manifested by a martensite increase from 27% to 95% at fracture (ϵ_F=0.32, σ_F=4000 MPa) at room temperature. The first stage of martensite formation occurs during plastic straining to 0.04-0.1 when the martensite increases from 27% to 70%. Further straining to fracture, within less than two wire diameters gage length, causes further transformation to nearly 100% martensite. The rotating beam fatigue endurance limit (1350 MPa) is higher than anticipated from the tensile strength, probably due to a significant amount of martensite formation in the failure zone. No martensite is formed for tension-tension cycling for 10,000 cycles and maximum stresses up to 862 MPa. For AM-355 CRT the fracture ductility decreases with increasing stress biaxiality from 0.6 for uniaxial tension to 0.2 for plane strain tension and bulge tests. In the bulge test the martensite content increases from 45 to 85% for a strain of 0.2. Increasing the strain rate causes an increase in the bulge ductility to 0.5 for explosive tests ($\dot{\epsilon} \sim 10^3$ sec^{-1}). The plane stress fracture toughness for AM-355 CRT was measured as approximately 100 $MNm^{-3/2}$ with the formation of approximately 20% martensite near the crack zone. Type 301 stainless steel (half hard grade) also showed significant increase in bulge ductility with increasing strain rate from 0.4 under quasi static loading to 0.8 under explosive ($\dot{\epsilon} \sim 10^3$ sec^{-4}) with a concomitant martensite transformation from approximately 20% to over 90%.

Syracuse University
Department of Chemical Engineering and
Materials Science
Syracuse, New York 13210
AD ______
UNCLASSIFIED
UNLIMITED DISTRIBUTION
THE RELATIONSHIPS BETWEEN THE TRANSFORMATION CHARACTERISTICS AND THE FRACTURE AND FATIGUE PROPERTIES OF TRIP STEELS AND OTHER METASTABLE AUSTENITIC STEELS
V. Weiss, K. Schroder, P. Sherman and A. Pan,
Syracuse University, Syracuse, N.Y. 13210
Final Report AMMRC CTR 77-1, January 1977, 49 pp.
illus - tables, Contract DAAG46-75-C-0065 D/A Proj:
1T162105AH84, AMCMS Code: 612105.11.148400 Final Report
March 19, 1975 to July 18, 1976.
Key Words
TRIP steels, High strength steels, Stainless steels, Fracture toughness, Transformation plasticity, Phase transformation, Mechanical Properties, Fatigue Properties
Transformation plasticity was studied in TRIP steel wire, AM-355 CRT stainless steel sheet and two grades of type 301 stainless steel sheet. In the partially cold worked TRIP steel wire (yield strength 2070 MPa, tensile strength 2325 MPa) transformation plasticity is manifested by a martensite increase from 27% to 95% at fracture (ϵ_F=0.32, σ_F=4000 MPa) at room temperature. The first stage of martensite formation occurs during plastic straining to 0.04-0.1 when the martensite increases from 27% to 70%. Further straining to fracture, within less than two wire diameters gage length, causes further transformation to nearly 100% martensite. The rotating beam fatigue endurance limit (1350 MPa) is higher than anticipated from the tensile strength, probably due to a significant amount of martensite formation in the failure zone. No martensite is formed for tension-tension cycling for 10,000 cycles and maximum stresses up to 862 MPa. For AM-355 CRT the fracture ductility decreases with increasing stress biaxiality from 0.6 for uniaxial tension to 0.2 for plane strain tension and bulge tests. In the bulge test the martensite content increases from 45 to 85% for a strain of 0.2. Increasing the strain rate causes an increase in the bulge ductility to 0.5 for explosive tests ($\dot{\epsilon} \sim 10^3$ sec^{-1}). The plane stress fracture toughness for AM-355 CRT was measured as approximately 100 $MNm^{-3/2}$ with the formation of approximately 20% martensite near the crack zone. Type 301 stainless steel (half hard grade) also showed significant increase in bulge ductility with increasing strain rate from 0.4 under quasi static loading to 0.8 under explosive ($\dot{\epsilon} \sim 10^3$ sec^{-4}) with a concomitant martensite transformation from approximately 20% to over 90%.

Syracuse University
Department of Chemical Engineering and
Materials Science
Syracuse, New York 13210
AD ______
UNCLASSIFIED
UNLIMITED DISTRIBUTION
THE RELATIONSHIPS BETWEEN THE TRANSFORMATION CHARACTERISTICS AND THE FRACTURE AND FATIGUE PROPERTIES OF TRIP STEELS AND OTHER METASTABLE AUSTENITIC STEELS
V. Weiss, K. Schroder, P. Sherman and A. Pan,
Syracuse University, Syracuse, N.Y. 13210
Final Report AMMRC CTR 77-1, January 1977, 49 pp.
illus - tables, Contract DAAG46-75-C-0065 D/A Proj:
1T162105AH84, AMCMS Code: 612105.11.148400 Final Report
March 19, 1975 to July 18, 1976.
Key Words
TRIP steels, High strength steels, Stainless steels, Fracture toughness, Transformation plasticity, Phase transformation, Mechanical Properties, Fatigue Properties
Transformation plasticity was studied in TRIP steel wire, AM-355 CRT stainless steel sheet and two grades of type 301 stainless steel sheet. In the partially cold worked TRIP steel wire (yield strength 2070 MPa, tensile strength 2325 MPa) transformation plasticity is manifested by a martensite increase from 27% to 95% at fracture (ϵ_F=0.32, σ_F=4000 MPa) at room temperature. The first stage of martensite formation occurs during plastic straining to 0.04-0.1 when the martensite increases from 27% to 70%. Further straining to fracture, within less than two wire diameters gage length, causes further transformation to nearly 100% martensite. The rotating beam fatigue endurance limit (1350 MPa) is higher than anticipated from the tensile strength, probably due to a significant amount of martensite formation in the failure zone. No martensite is formed for tension-tension cycling for 10,000 cycles and maximum stresses up to 862 MPa. For AM-355 CRT the fracture ductility decreases with increasing stress biaxiality from 0.6 for uniaxial tension to 0.2 for plane strain tension and bulge tests. In the bulge test the martensite content increases from 45 to 85% for a strain of 0.2. Increasing the strain rate causes an increase in the bulge ductility to 0.5 for explosive tests ($\dot{\epsilon} \sim 10^3$ sec^{-1}). The plane stress fracture toughness for AM-355 CRT was measured as approximately 100 $MNm^{-3/2}$ with the formation of approximately 20% martensite near the crack zone. Type 301 stainless steel (half hard grade) also showed significant increase in bulge ductility with increasing strain rate from 0.4 under quasi static loading to 0.8 under explosive ($\dot{\epsilon} \sim 10^3$ sec^{-4}) with a concomitant martensite transformation from approximately 20% to over 90%.

Syracuse University
Department of Chemical Engineering and
Materials Science
Syracuse, New York 13210
AD ______
UNCLASSIFIED
UNLIMITED DISTRIBUTION
THE RELATIONSHIPS BETWEEN THE TRANSFORMATION CHARACTERISTICS AND THE FRACTURE AND FATIGUE PROPERTIES OF TRIP STEELS AND OTHER METASTABLE AUSTENITIC STEELS
V. Weiss, K. Schroder, P. Sherman and A. Pan,
Syracuse University, Syracuse, N.Y. 13210
Final Report AMMRC CTR 77-1, January 1977, 49 pp.
illus - tables, Contract DAAG46-75-C-0065 D/A Proj:
1T162105AH84, AMCMS Code: 612105.11.148400 Final Report
March 19, 1975 to July 18, 1976.
Key Words
TRIP steels, High strength steels, Stainless steels, Fracture toughness, Transformation plasticity, Phase transformation, Mechanical Properties, Fatigue Properties
Transformation plasticity was studied in TRIP steel wire, AM-355 CRT stainless steel sheet and two grades of type 301 stainless steel sheet. In the partially cold worked TRIP steel wire (yield strength 2070 MPa, tensile strength 2325 MPa) transformation plasticity is manifested by a martensite increase from 27% to 95% at fracture (ϵ_F=0.32, σ_F=4000 MPa) at room temperature. The first stage of martensite formation occurs during plastic straining to 0.04-0.1 when the martensite increases from 27% to 70%. Further straining to fracture, within less than two wire diameters gage length, causes further transformation to nearly 100% martensite. The rotating beam fatigue endurance limit (1350 MPa) is higher than anticipated from the tensile strength, probably due to a significant amount of martensite formation in the failure zone. No martensite is formed for tension-tension cycling for 10,000 cycles and maximum stresses up to 862 MPa. For AM-355 CRT the fracture ductility decreases with increasing stress biaxiality from 0.6 for uniaxial tension to 0.2 for plane strain tension and bulge tests. In the bulge test the martensite content increases from 45 to 85% for a strain of 0.2. Increasing the strain rate causes an increase in the bulge ductility to 0.5 for explosive tests ($\dot{\epsilon} \sim 10^3$ sec^{-1}). The plane stress fracture toughness for AM-355 CRT was measured as approximately 100 $MNm^{-3/2}$ with the formation of approximately 20% martensite near the crack zone. Type 301 stainless steel (half hard grade) also showed significant increase in bulge ductility with increasing strain rate from 0.4 under quasi static loading to 0.8 under explosive ($\dot{\epsilon} \sim 10^3$ sec^{-4}) with a concomitant martensite transformation from approximately 20% to over 90%.